

Geochemical mapping of remote islands around Kyushu, Japan

Atsuyuki Ohta^{1,*}

Atsuyuki Ohta (2018) Geochemical mapping of remote islands around Kyushu, Japan. *Bull. Geol. Surv. Japan*, vol. 69 (5), p. 233–263, 11 figs, 6 tables.

Abstract: This paper describes high-density geochemical mapping of isolated islands in southwest Japan. A total of 193 stream sediments and three volcanic ash deposits collected from isolated islands around Kyushu were analyzed to determine the content of 53 elements to supplement land and sea geochemical mapping of the Kyushu area and regional Sr isotope mapping. The relationship between the spatial distribution of elements in stream sediments and volcanic ash deposits and the geology was closely examined using geographical information system (GIS) software. Stream sediments derived from mafic volcanic and pyroclastic rocks and volcanic ash deposits were enriched with MgO, CaO, Sc, TiO₂, V, T-Fe₂O₃, Co, and Sr. The presence of alkaline mafic volcanic rock increased the concentration of Cr, Ni, Nb, La, Ce, Pr, Nd, and Ta in stream sediments. Stream sediments originating from granitic rock were abundant in Be, Na₂O, K₂O, CaO, Sr, Y, Sn, Ln, Th, and U. Accretionary and non-accretionary sedimentary rocks caused an increase in Nb and Ta concentrations in stream sediments, and a reduction in Na₂O, MgO, CaO, and Sr concentrations. These geochemical features could be explained by the relative abundance of major rock forming minerals (such as quartz, plagioclase, K-feldspar, and mafic minerals) and accessory minerals (such as apatite and monazite) derived from the host rocks. Also, Zn-Pb deposits increased Zn, Cd, and Pb concentrations in stream sediments on Tsushima Island, and Sb deposits enhanced the Sb concentration in stream sediments on Amakusa-Shimoshima Island.

Keywords: stream sediment; geochemical map; isolated island; Kyushu; multi-element analysis

1. Introduction

Geochemical maps showing the regional distribution of element concentration at the Earth's surface, provide fundamental information about elements in nature and are used for mineral exploration and environmental assessment (Darnley *et al.*, 1995; Webb *et al.*, 1978). The Geological Survey of Japan, National Institute of Advanced Industrial Science and Technology (AIST), has created nationwide geochemical maps of Japan and the surrounding sea mainly for environmental assessment (Imai *et al.*, 2010; Imai *et al.*, 2004). As a next step, high-density geochemical mapping was conducted in the Kanto and Tokai areas, which have high population densities and are important industrial zones (Imai *et al.*, 2015). In addition, higher-density geochemical mapping of remote islands has been ongoing in order to supplement previously published land and sea geochemical maps of Japan (Ohta, 2018). In the present study, stream sediments and volcanic ash deposits were collected from 23 remote islands around Kyushu and the concentration of 53 elements was analyzed (Fig. 1). Geochemical maps of remote islands around Kyushu are very important for evaluating the influence of terrigenous

clastics on marine sediments in the Tsushima Strait and the East China Sea, which were collected far from mainland Kyushu, and for assessing the influence of specific rocks narrowly or sporadically distributed on the main islands of Japan on stream sediments. This study focuses on the geochemical features of stream sediments derived from Neogene-Quaternary alkaline volcanic rocks, Neogene granitic rocks, Paleogene sediments hosting coal deposits, and Cretaceous sedimentary rocks on remote islands. The results obtained in this study will contribute to future research on land and marine geochemical mapping and Sr isotope map in the Kyushu region.

2. Study area and samples

2.1 Geology

Figure 2 shows a geological map of the isolated islands in the Kyushu region, which has been simplified from a seamless digital geological map of Japan at a 1:200,000 scale (Geological Survey of Japan, AIST (ed.), 2015). Figure 2a shows that Paleogene-Neogene sediment is distributed mainly in the northern and southern parts of Tsushima Island. Neogene granitic rock and non-alkaline

¹ AIST, Geological Survey of Japan, Institute of Geology and Geoinformation

* Corresponding author: A. Ohta, Central 7,1-1-1 Higashi, Tsukuba, Ibaraki 305-8567, Japan. Email:a.ohta@aist.go.jp

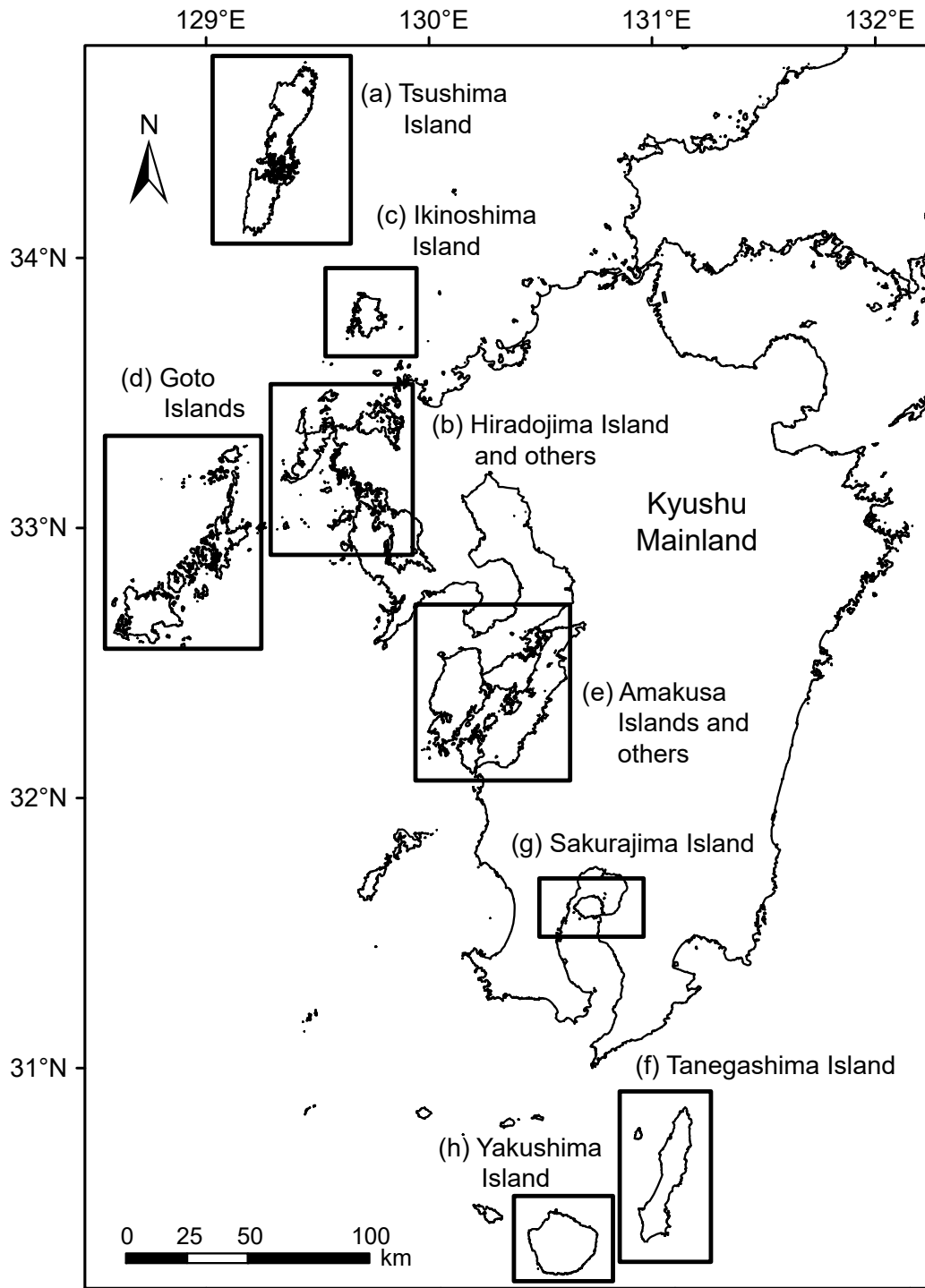


Fig. 1 Study area of remote islands around the Kyushu mainland. (a) Tsushima Island, (b) Takashima, Fukushima, Ikitsushima, Hiradojima, Oshima, and Matsushima Islands, (c) Ikinoshima Island, (d) Goto Islands (Ukujima, Ojikajima, Nakadorijima, Wakamatsujima, Hisakajima, and Fukuejima Islands), (e) Uto Peninsula, and Amakusa Islands (Oyanojima, Amakusa-kamishima, Amakusa-shimoshima, Goshorajima, Shishijima, and Nagashima Islands), (f) Tanegashima Island, (g) Sakurajima Island, (h) Yakushima Island.

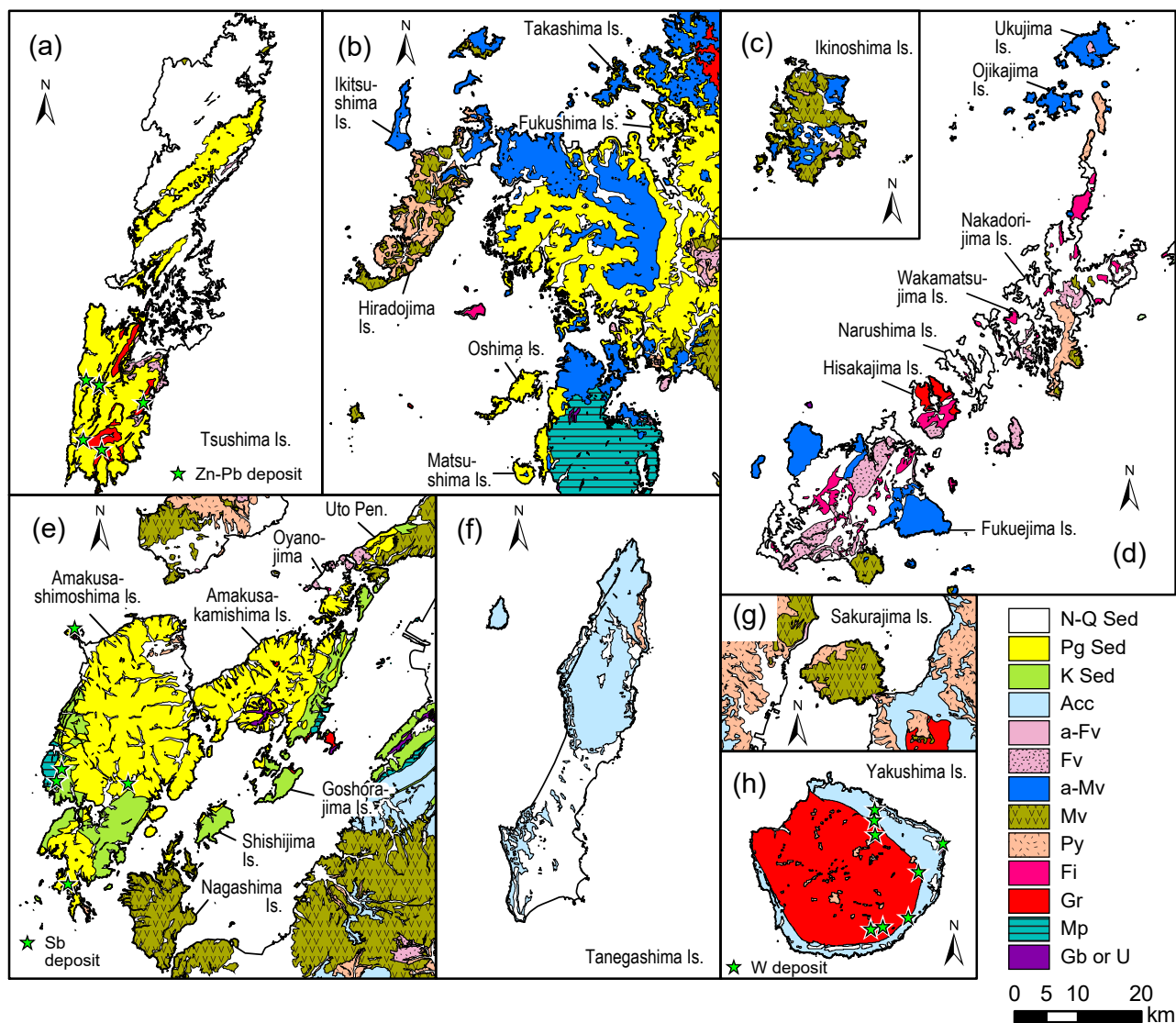


Fig. 2 Geological map for remote islands around the Kyushu mainland at a scale of 1:200,000 (Geological Survey of Japan, AIST (ed.), 2015). (a)-(h) same as Fig. 1. Star symbols indicate metalliferous deposits. N-Q Sed: Neogene and Quaternary sediment, Pg Sed: Paleogene sediment, K Sed: Cretaceous sedimentary rock, Acc: Paleogene Accretionary complex, a-Fv: Neogene alkaline felsic volcanic rock, Fv: Neogene non-alkaline felsic volcanic rock, a-Mv: Neogene and Quaternary alkaline mafic volcanic rock, Mv: Neogene and Quaternary non-alkaline mafic volcanic rock, Py: Neogene and Quaternary non-alkaline pyroclastic rock, Fi: Neogene non-alkaline felsic intrusive rock, Gr: Cretaceous and Neogene granitic rock, Mp: Cretaceous high-pressure metamorphic rock, Gb or U: Neogene gabbroic rock or ultramafic rock.

felsic volcanic rocks also are found in the southern part of Tsushima Island. Some metalliferous deposits, especially near the Taishu mine, yielding Cu, Zn, Pb, and Bi, are located around a granitic rock intrusion (Karakida *et al.*, 1992).

Figure 2b shows the geology in the northwest part of Kyushu Island. Neogene alkaline mafic volcanic rock and Paleogene-Neogene sediment are found on Takashima, Fukushima, and Ikitushima Islands. The northeast part of Hiradojima Island is covered by Neogene alkaline mafic volcanic rock. The rest of the region is underlain with Neogene non-alkaline mafic volcanic rock and pyroclastic rock. Paleogene-Neogene sediment is distributed on

Oshima and Matsushima Islands. Ikinoshima Island is composed mainly of Neogene non-alkaline volcanic rocks and Quaternary alkaline volcanic rock (Fig. 2c).

The geology of the Goto Islands is shown in Fig. 2d. Ukujima Island and Ojikajima Island are underlain by Neogene alkaline volcanic rock and Quaternary alkaline volcanic rock (dominantly mafic rock), respectively. Nakadorijima and Wakamatsujima Islands are composed of Neogene sediments, Neogene non-alkaline felsic volcanic rock, Neogene non-alkaline pyroclastic rock, and Neogene non-alkaline felsic intrusive rocks. Hisakajima Island and Fukuejima Island contain Neogene-Quaternary unconsolidated sediments, Neogene non-alkaline felsic

volcanic and intrusive rock, and Neogene granitic rock. Furthermore, Quaternary alkaline mafic volcanic rock erupted in the northwest and southeast parts of Fukuejima Island.

Amakusa-kamishima, Amakusa-shimoshima, Goshorajima, and Shishijima Islands are dominantly covered by Paleogene sedimentary rock associated with coal-field and Cretaceous sedimentary rock (Karakida *et al.*, 1992) (Fig. 2e). Cretaceous high-pressure metamorphic rock (Nagasaki metamorphic rock) and Neogene gabbroic rock are found in the western portion of Amakusa-shimoshima Island and the south-central part of Amakusa-kamishima Island; however their exposed area is small. The star symbols on Amakusa-shimoshima Island are small Sb deposits (Karakida *et al.*, 1992). By contrast, Nagashima Island is composed of Neogene non-alkaline mafic volcanic rock. Paleogene and Neogene sediments are widely distributed on Oyanojima Island. Uto Peninsula is composed mainly of Quaternary non-alkaline mafic volcanic rock.

The dominant deposits on Sakurajima Island consist of Quaternary non-alkaline mafic volcanic rock and pyroclastic rock (Fig. 2g). The Paleogene accretionary complex, composed mainly of sedimentary rock, is distributed mainly in the northern part of Tanegashima Island, and Neogene and Quaternary unconsolidated sediment outcrops are found mainly in the southern part of Tanegashima Island (Fig. 2f). The central part of Yakushima Island is intruded by Neogene granitic rock while the outer areas are composed mainly of a Paleogene accretionary complex (Fig. 2h). The star symbols in Fig. 2h indicate tungsten (W) deposits (Karakida *et al.*, 1992).

2.2 Samples

From 2013 to 2014, 191 stream sediment samples were collected from 23 islands, two stream sediments were collected from Uto Peninsula, and three volcanic ash deposits were collected from Sakurajima Island (Fig. 3). The sampling locations are summarized in Table 1. The sampling density was one sample per 6–31 km², with a mean of 15 km², which is approximately one-seventh of that used for nationwide geochemical mapping (100–120 km²). All rivers on the remote islands, except for Yakushima Island, are maintained with revetment walls on both banks. Stream sediments were collected from the river bed, air-dried at room temperature over 2 to 3 weeks, and sieved through an 83 mesh (180 μm) screen. In addition, magnetic minerals were removed from the air-dried samples using a hand magnet to minimize the effect of magnetic mineral accumulation (Imai *et al.*, 2004). Table 1 also shows the relative weight ratio of grains with sizes of less than 180 μm to stream sediments with grain sizes of less than 2 mm. The ratio is about 3–6% in the most cases, but is extremely low for samples from Yakushima Island (generally less than 2%), and high for samples from Fukushima Island (9–15%), Matsushima Island (20%), Sakurajima Island (22–60%),

and Tanegashima Island (3–60%).

In addition, samples SK03, Tn02, Tn09, Tn26, Yk01, and Yk17 were further sieved using seven types of screens: 2 mm, 1 mm, 500 μm, 250 μm, 125 μm, 63 μm, and 32 μm. Coarser grains larger than 2 mm (gravel fraction) were not used in the present study. The sieved samples were ground with an agate mortar and pestle. The relative weight ratio for the different grain sizes to stream sediments less than 2 mm is shown in Table 2. About 60–94% of stream sediments smaller than 2 mm was composed of medium to very coarse-grained sand (larger than 250 μm), but the proportion for Sk03 was just 26%. The modal center was very coarse sand (1–2 mm) for Tn09, coarse sand (0.5–1 mm) for Yk17, medium sand (250–500 μm) for Sk03, Tn26, and Yk01, and fine sand (125–250 μm) for Tn02. The fine and very fine sand fractions (63–250 μm) were 20–37% of stream sediments less than 2 mm for Sk03, Tn02, Tn26, and Yk01, and only 4–10% for Tn09 and Yk17.

2.3 Watershed analyses

Stream sediments consist of the products of weathering and erosion of soil and rocks in the watershed area upstream of the sampling site (Howarth and Thornton, 1983). Therefore, the geochemistry of stream sediments is determined by the dominant lithology distributed in their water catchment area (Ohta *et al.*, 2004). The watershed area for each sampling location was obtained using a digital elevation model (50 m mesh data) obtained from the Geospatial Information Authority of Japan (GSI). Geographic information system software (ArcGIS 10.5; Environmental Systems Research Institute) was used for the calculation.

The representative lithology for each sample was defined as the rock type exposed most widely in a drainage basin. The detailed process of Ohta *et al.* (2004) was followed carefully. In this study, a total of 196 samples were classified into 13 subgroups on the basis of the dominant geology: Neogene–Quaternary sediment (N–Q Sed), Paleogene sediment (Pg Sed), Cretaceous sedimentary rock (K Sed), Paleogene accretionary complex composed mainly of sedimentary rocks (Acc), Neogene and Quaternary alkaline felsic and mafic volcanic rocks (a-Fv and a-Mv, respectively), Neogene and Quaternary non-alkaline felsic and mafic volcanic rocks (Fv and Mv, respectively), Neogene and Quaternary non-alkaline pyroclastic rock (Py), Neogene non-alkaline felsic intrusive rock (Fi), Neogene granitic rocks (Gr), Neogene gabbroic rock (Gb), and Cretaceous metamorphic rock composed mainly of high-pressure metamorphic rock (Mp). If no representative rock was present in the watershed, the sample was classified as other (Oth). Tables 3 and 4 summarize the relative exposed areas of these lithologies in each drainage basin for the northern and southern regions, respectively.

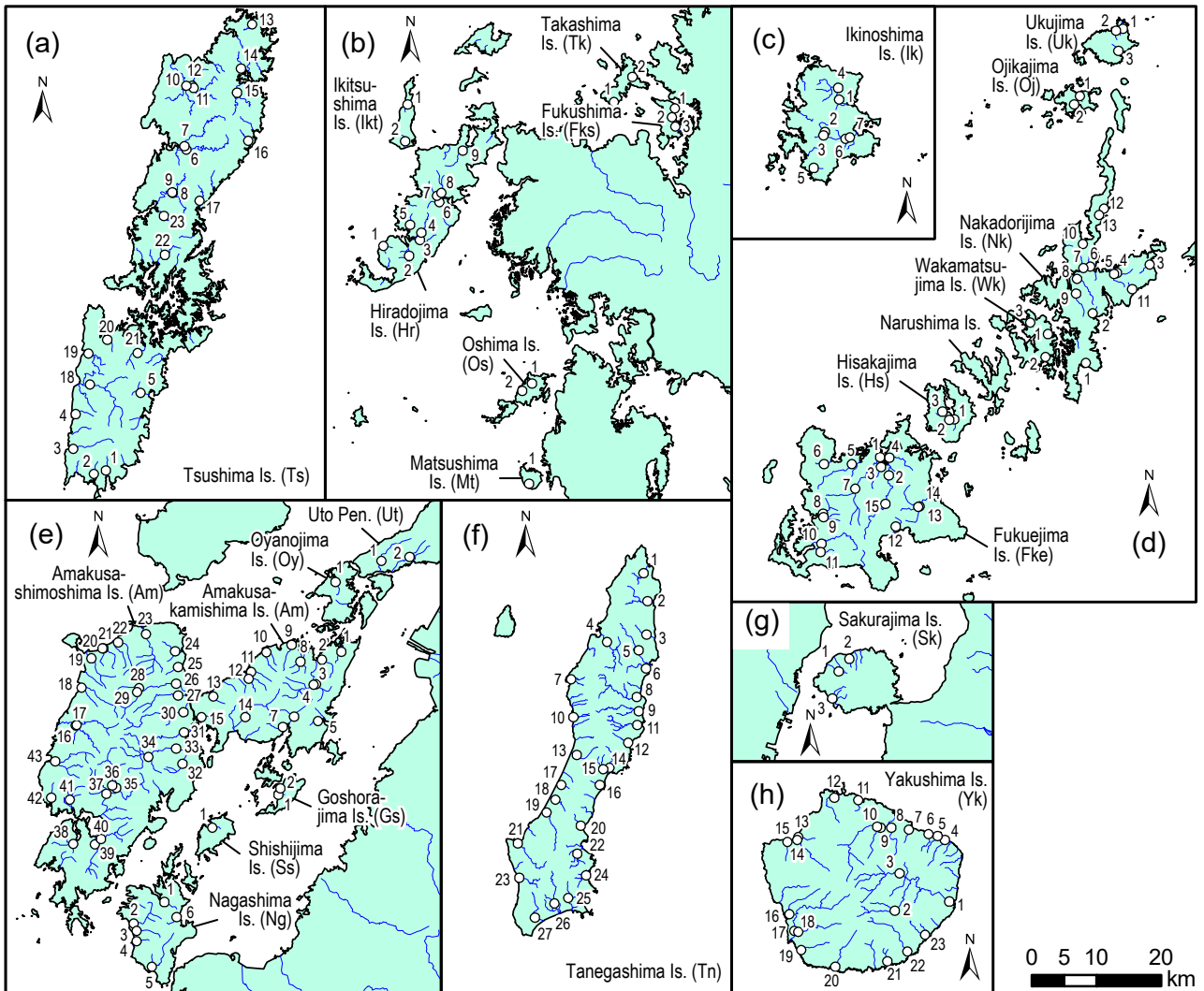


Fig. 3 Stream sediment sampling locations on remote islands around Kyushu mainland. (a)-(h) are the same as Fig. 1.

3. Analytical methods

The analytical methods of Ohta (2018) were followed for 53 elements in stream sediment samples. The amount of moisture (H_2O) was determined with 0.1 g of stream sediment sample after drying at $110^\circ C$ for 2 h. A thermally-dried sample (0.1 g) was digested using an HF, HNO_3 , and $HClO_4$ mixed solution at $125^\circ C$ for 2 h and $145^\circ C$ for 1 h. The digested product was evaporated to dryness at $190^\circ C$. The residue was dissolved in HNO_3 and diluted to 100 mL with double-deionized water. A solution of digested geochemical reference material JB-1a was used as a standard (Imai, 1990). In addition to the standard solution, a high concentration standard solution also was prepared from 1,000 mg/L solutions (Kanto Chemical Co. Inc.) for elemental analyses of samples having Li, Be, Cu, Zn, Cd, Mo, Sn, Sb, Cs, Tl, Pb, and Bi concentrations greater than ten times those of JB-1a (Ohta, 2018).

For As determination, 0.1 g of not thermally-dried

(undried) samples were digested using an HF, HNO_3 , and $HClO_4$ mixed solution with $KMnO_4$ at $120^\circ C$ for 20 min, a procedure modified from that reported by Terashima (1976, 1984). The degraded product was evaporated at $190^\circ C$ until the solution was ca. 1 mL. HCl was added to the residual solution, which was then heated at $135^\circ C$ for 30 min, and finally diluted to 100 mL with double-deionized water. A standard solution was prepared from a 1,000 mg/L arsenic atomic absorption standard solution (Kanto Chemical Co. Inc.).

Inductively coupled plasma atomic emission spectrometry (ICP-AES) (Thermo Fisher Scientific Inc., iCap 6300) was used to determine the Na, Mg, Al, P, K, Ca, Ti, Mn, Fe, Li, Be, V, Sr, and Ba concentrations. The major elements, Na, Mg, Al, P, K, Ca, Ti, Mn, and Fe, in stream sediments are expressed as oxides. The analytical wavelengths (nm) chosen were: Li (670.7), Be (313.1), Al (237.3), P (213.6), V (292.4), Ti (323.4), Mn (257.6), Sr (407.7), and Ba (455.4) using axial plasma viewing;

Table 1 Samples, places (islands), and rivers, along with locations and descriptions of samples and rivers.

Sample	Island	River	Longitude (JGD2000)	Latitude (JGD2000)	Sampling data	Width of river (m)	Depth of river (cm)	Flow rate of river	Ratio of <180 μm ^a
Ts01	Tsushima	対馬島 Nain	129°13'51.4"E	34°7'12.8"N	2013/10/9	4	20	1 m / 2 s	6.0%
Ts02	Tsushima	対馬島 Asamo	129°12'44.9"E	34°6'56.5"N	2013/10/9	8	20	1 m / 6 s	3.7%
Ts03	Tsushima	対馬島 Segawa	129°10'52.8"E	34°8'53.5"N	2013/10/9	20	n.d.	very slow	7.2%
Ts04	Tsushima	対馬島 Kotsuki	129°11'4.8"E	34°11'31.9"N	2013/10/9	6	20	1 m / 2 s	9.9%
Ts05	Tsushima	対馬島 Asu	129°17'4.1"E	34°13'8.5"N	2013/10/9	7	30	1 m / 4 s	10%
Ts06	Tsushima	対馬島 Kaidokoro	129°21'20.7"E	34°31'43.5"N	2013/10/10	8	>50	1 m / 4 s	2.4%
Ts07	Tsushima	対馬島 Nita	129°21'10.5"E	34°31'59"N	2013/10/10	7	n.d.	1 m / 5 s	13%
Ts08	Tsushima	対馬島 Sagauchi	129°20'3.2"E	34°28'24.2"N	2013/10/10	8	20	1 m / 6 s	2.7%
Ts09	Tsushima	対馬島 Mine	129°19'59.6"E	34°28'28.1"N	2013/10/10	6	100	1 m / 8 s	1.4%
Ts10	Tsushima	対馬島 Sago	129°21'54.4"E	34°36'36.5"N	2013/10/10	5	35	1 m / 10 s	3.7%
Ts11	Tsushima	対馬島 Sago	129°22'1.8"E	34°36'26.9"N	2013/10/10	8	30	1 m / 4 s	7.3%
Ts12	Tsushima	対馬島 Nakayama	129°21'20.9"E	34°36'36.6"N	2013/10/10	7	20	1 m / 2 s	1.8%
Ts13	Tsushima	対馬島 Toyokawa	129°27'27.5"E	34°41'16.8"N	2013/10/10	5	20	very slow	3.9%
Ts14	Tsushima	対馬島 Kusu	129°26'24.9"E	34°37'54.2"N	2013/10/10	20	40	1 m / 14 s	8.8%
Ts15	Tsushima	対馬島 Syushi	129°26'3.1"E	34°36'4"N	2013/10/10	12	40	1 m / 3 s	9.4%
Ts16	Tsushima	対馬島 Ashimi	129°27'3"E	34°32'22.4"N	2013/10/11	8	20	1 m / 8 s	1.2%
Ts17	Tsushima	対馬島 Saga	129°22'33.9"E	34°27'47.8"N	2013/10/11	4	30	1 m / 7 s	4.5%
Ts18	Tsushima	対馬島 Sasu	129°12'23.9"E	34°13'46.5"N	2013/10/11	20	>70	very slow	3.2%
Ts19	Tsushima	対馬島 Aren	129°12'17.4"E	34°16'9.4"N	2013/10/11	8	20	1 m / 3 s	2.4%
Ts20	Tsushima	対馬島 Kashi	129°13'58.7"E	34°17'11.2"N	2013/10/11	3	30	1 m / 3 s	1.3%
Ts21	Tsushima	対馬島 Sumo	129°16'47.8"E	34°16'10.9"N	2013/10/11	12	30	1 m / 4 s	6.2%
Ts22	Tsushima	対馬島 Ni-i	129°19'18"E	34°23'40.7"N	2013/10/11	6	30	very slow	3.9%
Ts23	Tsushima	対馬島 Yoshida	129°19'15.1"E	34°26'39.3"N	2013/10/11	5	40	1 m / 6 s	2.5%
Tk01	Takashima	鷹島 Tokonami	129°44'19.5"E	33°24'31.8"N	2014/10/10	2.5	20	1 m / 6 s	4.9%
Tk02	Takashima	鷹島 -	129°46'0.9"E	33°26'25.3"N	2014/10/10	0.7	3	1 m / 3 s	8.8%
Fks01	Fukushima	福島 -	129°49'52.3"E	33°23'59.7"N	2014/10/11	0.7	10	1 m / 3 s	13%
Fks02	Fukushima	福島 -	129°49'38.1"E	33°23'20.2"N	2014/10/11	2	10	1 m / 4 s	15%
Fks03	Fukushima	福島 -	129°49'56.5"E	33°22'36.6"N	2014/10/11	2.5	40	very slow	9.3%
lkt01	Ikitusushima	生月島 -	129°25'33.2"E	33°24'25.6"N	2014/10/9	4.5	<1	1 m / 4 s	7.0%
lkt02	Ikitusushima	生月島 Kaminogawa	129°25'16.9"E	33°21'36.8"N	2014/10/9	2	10	1 / 210 s	9.3%
Hr01	Hiradojima	平戸島 -	129°23'18.6"E	33°13'35.7"N	2014/10/9	2	10	1 m / 15 s	10%
Hr02	Hiradojima	平戸島 Kota	129°25'37.1"E	33°12'50.5"N	2014/10/9	2.5	20	1 m / 9 s	2.2%
Hr03	Hiradojima	平戸島 Shikisa	129°26'35.7"E	33°14'3.4"N	2014/10/9	2.5	15	1 m / 30 s	2.8%
Hr04	Hiradojima	平戸島 Nakatsura	129°26'43.8"E	33°14'36.3"N	2014/10/9	3	40	1 m / 10 s	4.9%
Hr05	Hiradojima	平戸島 -	129°25'41.9"E	33°15'12.8"N	2014/10/9	5	35	1 m / 10 s	3.2%
Hr06	Hiradojima	平戸島 Magome	129°28'25.6"E	33°16'56.6"N	2014/10/9	5	20	1 m / 11 s	3.0%
Hr07	Hiradojima	平戸島 Nakagawa	129°28'9.8"E	33°17'24.9"N	2014/10/9	5	35	1 m / 15 s	2.0%
Hr08	Hiradojima	平戸島 Yasuman	129°28'34.3"E	33°17'40.2"N	2014/10/9	8	70	1 m / 14 s	2.9%
Hr09	Hiradojima	平戸島 Kozone	129°30'31.7"E	33°20'52"N	2014/10/9	14	20	1 m / 10 s	3.0%
Os01	Oshima	大島 -	129°36'42.4"E	33°3'3.6"N	2014/10/8	1.5	3	1 m / 4 s	6.4%
Os02	Oshima	大島 -	129°35'48.2"E	33°2'28.9"N	2014/10/8	3	12	1 m / 16 s	7.5%
Mt01	Matsushima	松島 -	129°36'23.8"E	32°55'22.2"N	2014/10/8	0.7	6	1 m / 32 s	20%
lki01	Ikinoshima	老岐島 Tanie	129°44'12.9"E	33°48'46.4"N	2013/10/7	40	n.d.	n.d.	11%
lki02	Ikinoshima	老岐島 Hatahoko	129°42'52.6"E	33°46'18.2"N	2013/10/8	5	10	1 m / 6 s	1.9%
lki03	Ikinoshima	老岐島 Hatahoko	129°42'44.1"E	33°46'0.7"N	2013/10/8	3	25	1 m / 16 s	0.8%
lki04	Ikinoshima	老岐島 Tsunogawa	129°44'6.9"E	33°49'40.5"N	2013/10/8	4	10	1 m / 6 s	6.7%
lki05	Ikinoshima	老岐島 -	129°41'50.3"E	33°43'33.2"N	2014/10/7	V.C.	n.d.	n.d.	8.4%
lki06	Ikinoshima	老岐島 Ikeda	129°44'45.9"E	33°45'46.1"N	2014/10/7	4	35	very slow	2.9%
lki07	Ikinoshima	老岐島 Hatahoko	129°45'9.2"E	33°45'51.9"N	2014/10/7	10	10	1 m / 7 s	4.2%
Uk01	Ukujima	宇久島 -	129°7'57.6"E	33°17'24.7"N	2013/11/14	1	10	1 m / 3-4 s	4.7%
Uk02	Ukujima	宇久島 -	129°7'20.4"E	33°17'16.4"N	2013/11/14	3	10	1 m / 8 s	1.4%
Uk03	Ukujima	宇久島 Ebata	129°7'33.4"E	33°15'43.1"N	2013/11/14	3	10	1 m / 8 s	1.4%
Oj01	Ojikajima	小値賀島 -	129°4'4.6"E	33°12'17.1"N	2013/11/14	3.5	35	>1 m / 30 s	7.1%
Oj02	Ojikajima	小値賀島 -	129°3'31.7"E	33°11'38.5"N	2013/11/14	1.4	10	1 m / 4 s	3.1%
Nk01	Nakadorijima	中通島 -	129°4'35.6"E	32°51'53.3"N	2013/11/13	2	15	1 m / 10 s	5.3%
Nk02	Nakadorijima	中通島 -	129°5'13.2"E	32°55'40.7"N	2013/11/13	4	15	1 m / 11 s	2.7%
Nk03	Nakadorijima	中通島 -	129°10'22.7"E	32°59'23.4"N	2013/11/13	4	15	1 m / 7 s	5.8%
Nk04	Nakadorijima	中通島 Okawa	129°7'24.7"E	32°58'45.5"N	2013/11/13	6	30	1 m / 8 s	5.4%
Nk05	Nakadorijima	中通島 Kiba	129°7'7.9"E	32°58'40"N	2013/11/13	4	40	1 m / 13 s	3.2%
Nk06	Nakadorijima	中通島 Miyanogawa	129°5'0.6"E	32°59'13.8"N	2013/11/13	5	5	1 m / 4 s	2.9%
Nk07	Nakadorijima	中通島 Tsurido	129°4'21.6"E	32°59'6.8"N	2013/11/13	3	70	1 m / 15 s	6.4%
Nk08	Nakadorijima	中通島 Aiko	129°3'48.4"E	32°58'18.8"N	2013/11/13	8-10	40	very slow	21%
Nk09	Nakadorijima	中通島 Sanohara	129°3'43.1"E	32°57'11"N	2013/11/13	8	40-80	1 m / 25 s	1.9%
Nk10	Nakadorijima	中通島 -	129°4'20.4"E	33°0'58.2"N	2013/11/13	5	10	1 m / 7 s	5.3%
Nk11	Nakadorijima	中通島 -	129°8'46.6"E	32°57'30"N	2013/11/15	2	10	1 m / 5 s	6.3%
Nk12	Nakadorijima	中通島 -	129°6'15.7"E	33°3'39.5"N	2013/11/15	0.6	10	1 m / 6-8 s	5.3%
Nk13	Nakadorijima	中通島 -	129°5'48.3"E	33°3'10.1"N	2013/11/15	3	6	1 m / 6 s	4.0%
Wk01	Wakamatsujima	若松島 Suzuki	129°1'9.2"E	32°54'4.7"N	2013/11/15	2	15-20	1 m / 13 s	1.8%
Wk02	Wakamatsujima	若松島 -	129°0'55.1"E	32°52'18.6"N	2013/11/15	1.7	10	1 m / 1 s	5.3%
Wk03	Wakamatsujima	若松島 -	128°59'34.6"E	32°54'56.9"N	2013/11/15	2	15	1 m / 8 s	5.8%
Hs01	Hisakajima	久賀島 -	128°52'40.5"E	32°47'34.3"N	2013/11/12	6	50	very slow	5.8%
Hs02	Hisakajima	久賀島 Ichikogi	128°52'13.5"E	32°47'31.4"N	2013/11/12	10	10	1 m / 4 s	5.1%
Hs03	Hisakajima	久賀島 Inoki	128°51'36.9"E	32°48'9.7"N	2013/11/12	4	20	1 m / 8 s	6.2%
Fke01	Fukuejima	福江島 -	128°46'47.7"E	32°44'36.1"N	2013/11/11	7	20	1 m / 1 s	1.2%
Fke02	Fukuejima	福江島 Ichinokawa	128°46'45.3"E	32°43'15.6"N	2013/11/11	15	35	1 m / 4 s	0.8%
Fke03	Fukuejima	福江島 Uranogawa	128°46'1.6"E	32°43'53"N	2013/11/11	8	45	1 m / 8 s	2.4%
Fke04	Fukuejima	福江島 Wanigawa	128°45'56.1"E	32°44'39.1"N	2013/11/11	V.C.	n.d.	n.d.	25%

Table 1 continued.

Sample	Island	River	Longitude (JGD2000)	Latitude (JGD2000)	Sampling data	Width of river (m)	Depth of river (cm)	Flow rate of river	Ratio of <180 μm^a		
Tn12	Tanegashima	種子島	-	131°51'52.1"E	30°35'16.1"N	2014/12/4	4	15	1 m / 3 s	6.8%	
Tn13	Tanegashima	種子島	Owatase	大渡瀬川	130°57'17.3"E	30°34'22.4"N	2014/12/3	4	25	1 m / 4 s	7.3%
Tn14	Tanegashima	種子島	Mukai	向井川	131°0'12.9"E	30°33'21.3"N	2014/12/4	8	40-60	1 m / 5 s	5.0%
Tn15	Tanegashima	種子島	Tagiri	湧川	130°59'37.2"E	30°33'16.7"N	2014/12/4	8	35	1 m / 3 s	13%
Tn16	Tanegashima	種子島	-	130°59'18.2"E	30°32'2.8"N	2014/12/4	4	45	1 m / 5 s	11%	
Tn17	Tanegashima	種子島	-	130°55'53.7"E	30°32'7.7"N	2014/12/3	4	20	1 m / 3 s	5.2%	
Tn18	Tanegashima	種子島	Adakaiso	阿高磯川	130°55'21.9"E	30°30'59.8"N	2014/12/3	5	40-70	1 m / 15 s	9.8%
Tn19	Tanegashima	種子島	Kuhama	苦浜川	130°54'34.8"E	30°30'1"N	2014/12/3	15	60	very slow	18%
Tn20	Tanegashima	種子島	Imakumano	今熊野川	130°57'33.7"E	30°28'57.6"N	2014/12/4	5	15	1 m / 3 s	13%
Tn21	Tanegashima	種子島	Shimama	島間川	130°51'57.2"E	30°27'41.1"N	2014/12/3	5	35	1 m / 4 s	3.3%
Tn22	Tanegashima	種子島	Oura	大浦川	130°57'11.4"E	30°26'50.2"N	2014/12/4	20	N.D.	1 m / 4-5 s	60%
Tn23	Tanegashima	種子島	Okawa	大川	130°52'2.5"E	30°25'3.5"N	2014/12/3	6	35	1 m / 3 s	6.1%
Tn24	Tanegashima	種子島	Abusuki	阿武鋤川	130°57'55.6"E	30°25'10.8"N	2014/12/4	20	>60	very slow	31%
Tn25	Tanegashima	種子島	Miyase	宮瀬川	130°56'21.4"E	30°23'28.5"N	2014/12/3	6	60	1 m / 8 s	16%
Tn26	Tanegashima	種子島	Korigawa	郡川	130°55'7"E	30°23'4"N	2014/12/3	8	25	1 m / 3 s	11%
Tn27	Tanegashima	種子島	Shikanaki	鹿鳴川	130°53'21.6"E	30°22'1.3"N	2014/12/3	4	60	1 m / 9 s	11%
Sk01	Sakurajima	桜島	-	130°37'44.7"E	31°35'56.3"N	2014/11/10	V.C.	n.d.	n.d.	38%	
Sk02	Sakurajima	桜島	-	130°38'43.3"E	31°36'52.9"N	2014/11/10	V.C.	n.d.	n.d.	22%	
Sk03	Sakurajima	桜島	-	130°37'9.4"E	31°33'52.8"N	2014/11/10	V.C.	n.d.	n.d.	59%	
Yk01	Yakushima	屋久島	Anbo	安房川	130°39'4.1"E	30°18'57.1"N	2014/11/13	60-100	>100	n.d.	1.2%
Yk02	Yakushima	屋久島	Arakawa	荒川	130°34'16.1"E	30°18'16.9"N	2014/11/13	12	10-80	1 m / 3-5 s	0.4%
Yk03	Yakushima	屋久島	Anbo	安房川	130°34'43.2"E	30°21'8.3"N	2014/11/13	15	50	1 m / 5 s	0.7%
Yk04	Yakushima	屋久島	Menko	女川	130°38'46"E	30°23'38.4"N	2014/11/11	>16	>70	1 m / 4 s	13%
Yk05	Yakushima	屋久島	Ogako	男川	130°38'43.5"E	30°23'56.5"N	2014/11/15	3	25	1 m / 4 s	0.7%
Yk06	Yakushima	屋久島	Tabu	楯川	130°37'20.3"E	30°24'6.2"N	2014/11/11	>20	60	1 m / 5 s	0.4%
Yk07	Yakushima	屋久島	Jonogawa	城之川	130°35'38.2"E	30°24'27.7"N	2014/11/11	>3	40-50	1 m / 2-4 s	0.5%
Yk08	Yakushima	屋久島	Shiratani	白谷川	130°34'2.9"E	30°24'38"N	2014/11/14	8	50-70	1 m / 5 s	1.7%
Yk09	Yakushima	屋久島	Miyano-ura	宮之浦川	130°33'6.6"E	30°24'39.5"N	2014/11/11	>20	40	1 m / 5 s	2.7%
Yk10	Yakushima	屋久島	Miyano-ura	宮之浦川	130°32'46.9"E	30°24'45"N	2014/11/11	>30	60	1 m / 5 s	1.4%
Yk11	Yakushima	屋久島	Shidoko	志戸子川	130°31'11.6"E	30°26'47"N	2014/11/15	8	45	1 m / 9 s	0.5%
Yk12	Yakushima	屋久島	Isso	一湊川	130°29'4.7"E	30°26'59.1"N	2014/11/14	50	20	1 m / 22 s	1.2%
Yk13	Yakushima	屋久島	Domen	土面川	130°25'51"E	30°24'0.8"N	2014/11/15	20	15	1 m / 5 s	2.4%
Yk14	Yakushima	屋久島	Nagata	永田川	130°25'44.4"E	30°23'47.8"N	2014/11/14	50	70	1 m / 12 s	1.5%
Yk15	Yakushima	屋久島	Takeno	嶽之川	130°24'54.3"E	30°23'39.4"N	2014/11/14	6-8	40-100	1 m / 4-5 s	1.3%
Yk16	Yakushima	屋久島	Okogawa	大川	130°24'59.1"E	30°18'6.9"N	2014/11/15	12	40-70	1 m / 3-6 s	7.0%
Yk17	Yakushima	屋久島	Koyoji	小揚子川	130°25'23.1"E	30°16'51.3"N	2014/11/12	>50	60	1 m / 11 s	3.2%
Yk18	Yakushima	屋久島	Kurio	栗生川	130°25'43.3"E	30°16'46.7"N	2014/11/12	30	70	1 m / 5 s	0.9%
Yk19	Yakushima	屋久島	Nakama	中間川	130°25'58.4"E	30°15'21.9"N	2014/11/12	16	25	1 m / 4 s	0.3%
Yk20	Yakushima	屋久島	Yukawa	湯川	130°28'57"E	30°14'3.2"N	2014/11/12	>20	50	1 m / 11 s	0.7%
Yk21	Yakushima	屋久島	Futamata	二又川	130°33'33.9"E	30°14'24.7"N	2014/11/15	4	45	1 m / 6 s	0.8%
Yk22	Yakushima	屋久島	Tainogawa	鱧ノ川	130°35'20.5"E	30°15'9.2"N	2014/11/12	>40	40	1 m / 3-4 s	0.4%
Yk23	Yakushima	屋久島	Kodakumi	小田渡川	130°36'54.4"E	30°16'23.6"N	2014/11/15	4	90	1 m / 4-5 s	2.2%

V.C.: Vacant channel, n.d.: not determined

^a Relative ratio by weight of the <180 μm fraction to sediments less than 2 mm

Table 2 Relative weight ratio of grain size to stream sediments less than 2 mm.

Grain size	Sk03	Tn02	Tn09	Tn26	Yk01	Yk17
<180 μm	59%	22%	7.2%	11%	1.2%	3.2%
Very coarse sand (1-2 mm)	0.3%	20%	39%	12%	5.5%	31%
Coarse sand (0.5-1 mm)	5.7%	19%	28%	14%	15%	44%
Medium sand (250-500 μm)	20%	23%	20%	43%	38%	19%
Fine sand (125-250 μm)	12%	26%	7.9%	28%	33%	4%
Very fine sand (63-125 μm)	8.1%	6.7%	2.4%	2.1%	4.1%	0.4%
Coarse silt (32-63 μm)	3.4%	2.3%	1.2%	0.6%	0.4%	0.2% ^a
Fine silt and clay (<32 μm)	3.1%	1.9%	0.8%	0.4%	0.2%	

^a Grain size less than 63 μm

Table 3 Watershed area and estimated ratios of exposed lithology areas in each watershed for samples collected from the northern region of the study area.

Sample	Watershed area (km ²)							Sample	Watershed area (km ²)							Dominant lithology		
	Sed	a-Fv	Fv	a-Mv	Mv	Py	Fi		Gr	Sed	a-Fv	Fv	a-Mv	Mv	Py		Fi	Gr
Ts01	5.0	74%	-	-	-	-	-	-	26%	Sed	3.7	42%	-	37%	20%	1%	-	Mv+a-Mv
Ts02	4.9	74%	-	-	-	-	-	26%	Sed	Ik04	3.0	2%	2%	60%	36%	-	-	a-Mv
Ts03	16.4	48%	-	-	-	-	-	52%	Gr	Ik05	1.7	-	-	100%	-	-	-	Mv
Ts04	6.4	89%	6%	-	2%	-	-	3%	Sed	Ik06	2.7	10%	-	68%	-	-	-	Mv
Ts05	5.7	100%	-	-	-	-	-	-	Sed	Ik07	22.0	39%	2%	27%	30%	2%	-	Mv+a-Mv
Ts06	25.9	98%	2%	-	<1%	-	-	-	Sed	Uk01	1.2	-	-	100%	-	-	-	a-Mv
Ts07	24.7	96%	4%	-	<1%	-	-	-	Sed	Uk02	1.7	-	1%	99%	-	-	-	a-Mv
Ts08	8.9	92%	7%	-	1.0%	-	-	-	Sed	Uk03	1.8	<1%	52%	48%	-	-	-	a-Fv
Ts09	8.9	97%	3%	-	-	-	-	-	Sed	Oj01	0.15	-	-	100%	-	-	-	a-Mv
Ts10	4.8	100%	-	-	-	-	-	-	Sed	Oj02	0.5	-	-	100%	-	-	-	a-Mv
Ts11	15.1	98%	-	-	2%	-	-	-	Sed	Nk01	0.8	-	-	-	25%	75%	-	Py
Ts12	21.9	100%	-	-	<1%	-	-	-	Sed	Nk02	0.8	71%	-	29%	-	-	-	Sed
Ts13	2.5	100%	-	-	-	-	-	-	Sed	Nk03	2.8	68%	16%	16%	6%	-	-	Sed
Ts14	5.5	100%	-	-	-	-	-	-	Sed	Nk04	3.9	70%	9%	-	-	-	-	Sed
Ts15	10.6	96%	4%	-	-	-	-	-	Sed	Nk05	4.0	74%	-	-	13%	-	-	Sed
Ts16	3.2	100%	-	-	<1%	-	-	-	Sed	Nk06	1.2	85%	-	-	15%	-	-	Sed
Ts17	4.4	85%	15%	-	-	-	-	-	Sed	Nk07	4.2	99%	-	-	1%	-	-	Sed
Ts18	33.7	83%	7%	-	<1%	-	-	10%	Sed	Nk08	6.9	50%	48%	-	3%	-	-	Sed
Ts19	10.6	94%	5%	-	-	-	-	<1%	Sed	Nk09	6.2	25%	-	37%	-	37%	-	Fv+Py
Ts20	5.6	94%	3%	-	<1%	-	-	2%	Sed	Nk10	1.7	98%	-	-	2%	-	-	Sed
Ts21	9.8	56%	27%	-	-	-	-	17%	Sed	Nk11	1.5	80%	13%	-	-	-	-	Sed
Ts22	7.4	100%	-	-	-	-	-	-	Sed	Nk12	0.9	-	-	-	-	-	-	Fi
Ts23	4.9	93%	7%	-	-	-	-	-	Sed	Nk13	0.8	13%	-	-	-	-	-	Fi
Tr01	0.6	41%	-	-	59%	-	-	-	a-Mv	Wk01	1.9	68%	32%	-	-	-	-	Sed
Tr02	0.5	26%	-	-	74%	-	-	-	a-Mv	Wk02	0.5	23%	77%	-	-	-	-	Fv
Fks01	0.4	28%	-	-	72%	-	-	-	a-Mv	Wk03	0.8	60%	-	-	-	-	-	Sed
Fks02	1.0	50%	-	-	50%	-	-	-	Sed	Hs01	3.9	14%	25%	-	-	-	40%	<1%
Fks03	0.8	71%	-	-	19%	-	-	-	Sed	Hs02	3.5	15%	15%	-	-	-	60%	Fi
Ik01	0.7	-	-	-	100%	-	-	-	a-Mv	Hs03	3.5	55%	-	-	-	-	70%	Fi
Ik02	1.1	-	-	-	100%	-	-	-	a-Mv	Fke01	6.3	43%	49%	-	-	-	21%	Sed
Hr01	1.6	-	-	-	44%	56%	-	-	Py	Fke02	26.5	62%	27%	-	-	-	8%	Oth
Hr02	3.8	17%	-	-	32%	51%	-	-	Py	Fke03	5.0	52%	-	-	-	-	12%	Sed
Hr03	4.3	5%	-	-	19%	76%	-	-	Py	Fke04	32.0	36%	19%	24%	-	-	48%	Sed
Hr04	7.3	16%	-	-	22%	62%	-	-	Py	Fke05	11.1	100%	-	-	-	-	21%	Oth
Hr05	3.2	14%	-	-	15%	71%	-	-	Py	Fke06	4.1	21%	-	-	-	-	-	Sed
Hr06	4.5	9%	-	-	22%	68%	-	-	Py	Fke07	23.8	53%	12%	-	-	-	35%	Sed
Hr07	3.8	23%	-	-	63%	14%	-	-	Mv	Fke08	6.3	-	100%	-	-	-	-	Fv
Hr08	6.0	20%	-	-	3%	42%	-	-	Mv+Py	Fke09	5.2	72%	4%	-	-	-	23%	Sed
Hr09	7.1	42%	-	-	12%	33%	13%	-	Mv+Py	Fke10	14.5	46%	52%	-	-	-	2%	Fv
Os01	0.8	100%	-	-	-	-	-	-	Sed	Fke11	5.1	39%	61%	-	-	-	<1%	Fv
Os02	0.8	100%	-	-	-	-	-	-	Sed	Fke12	2.4	96%	-	3%	-	-	<1%	Sed
Mt01	0.3	100%	-	-	<1%	-	-	-	Sed	Fke13	2.1	14%	-	86%	-	-	-	a-Mv
Ik101	21.6	5%	3%	-	33%	59%	-	-	Mv	Fke14	12.1	69%	1%	21%	-	-	9%	Sed
Ik02	4.4	56%	-	-	27%	16%	2%	-	Sed	Fke15	16.0	79%	11%	-	-	-	10%	Sed

Sed: Paleogene-Neogene-Quaternary sediment, a-Fv: Neogene alkaline felsic volcanic rock, Fv: Neogene non-alkaline felsic volcanic rock, a-Mv: Neogene-Quaternary alkaline mafic volcanic rock, Mv: Neogene non-alkaline mafic volcanic rock, Py: Neogene-Quaternary pyroclastic rock, debris, and tephra, Fi: Neogene felsic intrusive rock, Gr: Neogene granitic rocks, Oth: other rocks.

Table 4 Watershed area and estimated ratio of exposed area of lithology to watershed area for samples collected from the southern region of the study area.

Sample	Watershed area (km ²)	Sed	K Sed	Acc	Mv	Py	Fi	Gr	Gb	Mp	Dominant lithology	Sample	Watershed area (km ²)	Sed	K Sed	Acc	Mv	Py	Fi	Gr	Gb	Mp	Dominant lithology
U01	8.1	39%	11%	-	50%	-	-	-	-	-	Mv	Tn01	5.7	3%	-	97%	-	-	<1%	-	-	-	Acc
U02	3.9	11%	-	-	89%	-	-	-	-	-	Mv	Tn02	16.7	2%	-	97%	-	<1%	2%	-	-	-	Acc
Oy01	2.5	100%	-	-	-	-	-	-	-	-	Sed	Tn03	3.8	<1%	-	89%	-	11%	-	-	-	-	Acc
Am01	3.2	36%	64%	-	-	-	-	-	-	-	K Sed	Tn04	18.8	24%	-	77%	-	-	-	-	-	-	Acc
Am02	6.0	55%	45%	-	-	-	-	-	-	-	Sed	Tn05	12.9	27%	-	69%	-	4%	-	-	-	-	Acc
Am03	6.1	49%	51%	-	-	-	-	-	-	-	K Sed	Tn06	4.9	12%	-	89%	-	-	-	-	-	-	Acc
Am04	17.4	100%	-	-	-	-	-	-	<1%	-	Sed	Tn07	3.5	3%	-	95%	-	-	2%	-	-	-	Acc
Am05	3.0	18%	81%	-	-	-	-	1%	-	-	K Sed	Tn08	17.4	8%	-	92%	-	-	-	-	-	-	Acc
Am06	8.7	96%	-	-	-	-	-	-	4%	-	Sed	Tn09	12.7	2%	-	98%	-	-	-	-	-	-	Acc
Am07	3.2	63%	-	-	-	-	-	-	37%	-	Sed	Tn10	3.2	6%	-	94%	-	-	-	-	-	-	Acc
Am08	5.4	100%	-	-	-	-	-	-	<1%	-	Sed	Tn11	9.5	1%	-	99%	-	-	-	-	-	-	Acc
Am09	3.2	100%	-	-	-	-	-	-	<1%	-	Sed	Tn12	4.7	3%	-	97%	-	-	-	-	-	-	Acc
Am10	3.0	90%	-	-	-	-	-	9%	-	-	Sed	Tn13	3.9	34%	-	66%	-	-	-	-	-	-	Acc
Am11	5.9	99%	-	-	-	-	-	-	1%	-	Sed	Tn14	8.5	30%	-	70%	-	-	-	-	-	-	Acc
Am12	9.1	100%	-	-	-	-	-	-	<1%	-	Sed	Tn15	6.4	42%	-	58%	-	-	-	-	-	-	Acc
Am13	3.3	98%	-	-	-	-	-	-	2%	-	Sed	Tn16	4.2	95%	-	5%	-	-	-	-	-	-	Sed
Am14	18.6	89%	-	-	-	-	-	-	11%	-	Sed	Tn17	2.6	86%	-	14%	-	-	-	-	-	-	Sed
Am15	3.9	100%	-	-	-	-	-	-	-	-	Sed	Tn18	7.6	84%	-	16%	-	-	-	-	-	-	Sed
Am16	11.8	63%	35%	-	-	-	-	-	-	-	Sed	Tn19	10.3	79%	-	21%	-	-	-	-	-	-	Sed
Am17	19.0	99%	<1%	-	-	-	-	-	-	-	Sed	Tn20	3.7	93%	-	7%	-	-	-	-	-	-	Sed
Am18	14.0	100%	-	-	-	-	-	-	<1%	-	Sed	Tn21	10.7	62%	-	38%	-	-	-	-	-	-	Sed
Am19	8.7	100%	-	-	-	-	-	-	<1%	-	Sed	Tn22	8.5	97%	-	3%	-	-	-	-	-	-	Sed
Am20	5.0	100%	-	-	-	-	-	-	<1%	-	Sed	Tn23	7.0	80%	-	20%	-	-	-	-	-	-	Sed
Am21	2.8	100%	-	-	-	-	-	-	<1%	-	Sed	Tn24	4.5	100%	-	-	-	-	-	-	-	-	Sed
Am22	6.4	100%	-	-	<1%	-	-	-	<1%	-	Sed	Tn25	5.7	94%	-	6%	-	-	-	-	-	-	Sed
Am23	27.8	97%	-	-	-	3%	-	-	<1%	-	Sed	Tn26	12.6	99%	-	2%	-	-	-	-	-	-	Sed
Am24	4.4	89%	-	-	-	11%	-	-	-	-	Sed	SK01	N.D.	-	-	-	-	100%	-	-	-	Py	
Am25	3.9	100%	-	-	-	-	-	-	-	-	Sed	SK02	N.D.	-	-	-	-	100%	-	-	-	Py	
Am26	25.8	100%	-	-	-	<1%	-	-	<1%	-	Sed	SK03	N.D.	-	-	-	-	100%	-	-	-	Py	
Am27	12.3	100%	-	-	-	-	-	-	<1%	-	Sed	Tn27	6.4	92%	-	8%	-	-	-	93%	-	-	Sed
Am28	8.5	100%	-	-	-	-	-	-	<1%	-	Sed	Yk01	84.1	<1%	-	2%	-	-	-	96%	-	-	Gr
Am29	8.1	100%	-	-	-	-	-	-	-	-	Sed	Yk02	13.2	1%	-	-	-	-	96%	-	-	-	Gr
Am30	22.5	100%	-	-	-	-	-	-	-	-	Sed	Yk03	29.5	1%	-	-	-	-	93%	-	-	-	Gr
Am31	9.9	100%	-	-	-	-	-	-	-	-	Sed	Yk04	7.9	4%	-	-	-	7%	-	6%	-	-	Acc
Am32	11.1	100%	-	-	<1%	-	-	-	-	-	Sed	Yk05	1.9	8%	-	87%	-	3%	-	-	-	-	Acc
Am33	31.1	100%	-	-	-	-	-	-	-	-	Sed	Yk06	5.7	2%	-	92%	-	<1%	-	10%	-	-	Acc
Am34	19.2	100%	-	-	-	-	-	-	-	-	Sed	Yk07	3.8	1%	-	72%	-	-	27%	-	-	-	Acc
Am35	17.8	94%	6%	-	<1%	-	-	-	-	-	Sed	Yk08	12.7	<1%	-	10%	-	4%	-	87%	-	-	Gr
Am36	17.7	100%	-	-	-	-	-	-	<1%	-	Sed	Yk09	8.3	-	-	<1%	-	4%	-	96%	-	-	Gr
Am37	12.1	99%	-	-	<1%	-	-	-	1%	-	Sed	Yk10	37.3	<1%	-	5%	-	2%	-	92%	-	-	Gr
Am38	5.7	49%	51%	-	<1%	-	-	-	-	-	K Sed	Yk11	6.6	2%	-	64%	-	1%	-	33%	-	-	Acc
Am39	12.1	42%	58%	-	<1%	-	-	-	<1%	-	K Sed	Yk12	12.6	2%	-	20%	-	5%	-	74%	-	-	Acc
Am40	10.0	3%	97%	-	-	-	-	-	-	-	K Sed	Yk13	4.5	-	-	-	-	1%	-	99%	-	-	Gr
Am41	8.8	69%	31%	-	-	-	-	-	-	-	Sed	Yk14	30.5	1%	-	-	-	2%	-	96%	-	-	Gr
Am42	4.9	2%	28%	-	<1%	-	-	-	-	69%	Mp	Yk15	7.3	3%	-	-	-	<1%	-	97%	-	-	Gr
Am43	18.3	77%	19%	-	<1%	-	-	-	-	1%	Sed	Yk16	11.3	-	-	-	-	3%	-	95%	-	-	Gr
Gs01	0.9	-	100%	-	-	-	-	-	-	-	K Sed	Yk17	28.1	-	-	-	-	6%	-	90%	-	-	Gr
Gs02	0.8	-	100%	-	-	-	-	-	-	-	K Sed	Yk18	20.7	-	-	-	-	2%	-	93%	-	-	Gr
Ss01	0.8	1%	99%	-	-	-	-	-	-	-	K Sed	Yk19	11.8	<1%	-	16%	-	<1%	-	84%	-	-	Gr
Ng01	3.4	8%	-	-	92%	-	-	-	-	-	Mv	Yk20	10.5	4%	-	7%	-	<1%	-	89%	-	-	Gr
Ng02	11.3	11%	-	-	89%	-	-	-	-	-	Mv	Yk21	2.7	<1%	-	6%	-	<1%	-	93%	-	-	Gr
Ng03	4.2	7%	-	-	93%	-	-	-	-	-	Mv	Yk22	17.2	-	-	2%	-	4%	-	94%	-	-	Gr
Ng04	3.7	5%	-	-	88%	-	-	-	-	-	Mv	Yk23	5.9	-	-	5%	-	2%	-	93%	-	-	Gr
Ng05	12.2	12%	-	-	93%	-	-	-	-	-	Mv												
Ng06	3.0	7%	-	-	93%	-	-	-	-	-	Mv												

Sed: Paleogene-Neogene-Quaternary sediment, K Sed: Cretaceous sedimentary rock, Mv: Neogene non-alkaline mafic volcanic rock, Py: Neogene-Quaternary pyroclastic rock, debris, and tephra, Fi: Miocene felsic intrusive rock, Gr: Neogene granitic rocks, Gb: Neogene gabbroic rocks, Mp: Cretaceous high-pressure type metamorphic rock.

and Na (589.5), Mg (202.5), K (766.4), Ca (315.8), and Fe (259.9) using radial plasma viewing. An ICP mass spectrometer (ICP-MS) (Agilent Technologies Inc., 7500ce) equipped with a He collision cell was used to determine the concentration of 38 elements. The elements and isotopes chosen for analysis were: Sc (45), Cr (53), Co (59), Ni (60), Cu (63), Zn (66), Ga (71), As (75), Rb (85), Y (89), Zr (90), Nb (93), Mo (95), Cd (111), Sn (120), Sb (121), Cs (133), La (139), Ce (140), Pr (141), Nd (146), Sm (147), Eu (151), Gd (157), Tb (159), Dy (163), Ho (165), Er (167), Tm (169), Yb (173), Lu (175), Hf (178), Ta (181), Tl (205), Pb (208), Bi (209), Th (232), and U (238). Although Pb isotope ratios in stream sediments change depending on the source rock, the quantitative values of Pb concentration obtained by ICP-MS were consistent with those determined by ICP-AES (Ohta, 2018).

The mercury concentration in undried samples was determined using an atomic absorption spectrometer that measured the quantity of Hg vapor generated from direct thermal decomposition of samples (Nihon Instruments Corp.; MA-2000). A standard solution prepared from a 1,000 mg/L mercury standard solution (Kanto Chemical Co. Inc.) was used to obtain the calibration curve. A wavenumber of 253.7 nm was used for determining the Hg concentration.

Quality control for the ICP-AES and ICP-MS analyses involved two geochemical reference samples, JB-1a and JB-3 (Imai *et al.*, 1995), which were inserted at the rate of 1 for every 5 and 10 samples, respectively. The geochemical reference sample JSI-1 (Imai *et al.*, 1996) was used for quality control of As and Hg determination and inserted at a rate of 1 for every 10 samples. Table 5 summarizes the analytical results for 53 elements in fine stream sediments (<180 μm) collected from remote islands around Kyushu. Element concentrations for SK03, Tn02, Tn09, Tn26, Yk01, and Yk17 samples, grouped into 7 grain sizes, are shown in Table 6. The As and Hg concentrations were recalculated as concentration per 1 kg of the thermally dried samples. The Zr and Hf concentrations were used only as a guide because the heavy mineral fraction, especially zircon, was not digested by the HF-HNO₃-HClO₄ solution.

The relative standard deviation (RSD) of the element concentration obtained from repeated measurements ($n = 3$) for Ts02, Fke07, Hr04, Am23, Tn02, and Yk01 samples was within $\pm 2\%$ for major elements, within $\pm 5\%$ for many minor elements, within $\pm 10\%$ for H₂O⁻, Li, Be, V, Cu, Zn, As, Nb, Ta, and Bi, and within $\pm 15\text{--}20\%$ for Sc, Cr, Mo, Cd, and Sb. The largest RSDs for Sn and Hg were within $\pm 100\%$ and $\pm 40\%$, respectively, perhaps due to heterogeneity of the Sn minerals (such as cassiterite) and Hg minerals (such as native Hg and cinnabar).

4. Results and discussion

4.1 Dependence of element concentration in stream sediments on grain size

Figure 4 shows the grain size dependence of the Al₂O₃, K₂O, CaO, TiO₂, T-Fe₂O₃, Cr, Cu, Y, Cd, Cs, La, and Pb concentration for Sk03, Tn02, Tn09, Tn26, Yk01, and Yb17. The Sk03 sample originated from Quaternary mafic pyroclastic rock, Tn02 and Tn09 originated from a Paleogene accretionary complex, Tn26 originated from Neogene sediment, and Yk01 and Yk17 originated from Neogene granitic rock. The concentration of most elements in Sk03 was similar regardless of grain size, which suggests that sand-sized particles formed the agglutinate of silty-sized volcanic ash fall in Sk03.

The chemical composition variations for Tn02, Tn09, and Tn26 were similar across grain size. Concentrations of many elements in Tn02, Tn09, and Tn26 decreased with decreasing grain size from the very coarse sand fraction (1–2 mm) to the fine sand fraction (125–250 μm), and then increased with a further decrease in grain size. This is called a V-shaped pattern. The CaO and Sr concentrations were largest in the coarse sand fractions (500–1000 μm), and then sharply decreased in the fine fractions (<250 μm). Their systematic variation across grain size was controlled dominantly by the abundance of plagioclase in clastics. The coarse and medium sand fractions (250–1000 μm) in Tn09 and the very fine fraction (63–125 μm) in Tn26 had the greatest concentrations of MgO, Sc, TiO₂, V, MnO, T-Fe₂O₃, and Co. These concentrations were influenced by the abundance of mafic minerals (olivine, pyroxene, amphibole, and biotite) and opaque minerals (magnetite and ilmenite). Enrichment of many elements in the finer stream sediments has been reported by Imai (1987) and Terashima *et al.* (2008), and was caused mainly by an increase in layer silicates (mainly clay minerals) containing Al₂O₃ and alkali metal elements, an increase in organic compounds bonding with heavy metals, and a less effective dilution effect with quartz that was less abundant in the finer fraction.

In contrast, the Be, Na₂O, Al₂O₃, CaO, and Sr concentrations in Yk01 and Yk17 samples increased gradually with decreasing grain size. These element concentrations, except for Al₂O₃, reached a maximum for the very fine sand fraction (63–125 μm) or the coarse silt fraction (32–63 μm). Systematic variations in CaO and Sr in these samples were opposite to those in Tn02, Tn09, and Tn26. Plagioclase appeared to be abundant in the fine sand fraction originating from granitic rock in Yakushima Island. The variations in the Li, K₂O, Rb, and Cs concentrations with grain size show a V-shaped pattern: the fine sand fraction (125–250 μm) or the very fine fractions (63–125 μm) had the lowest concentration. The steep decreases in K₂O and Rb concentrations with decreasing grain size can be explained by resistance of K-feldspar to weathering because the physical disruption of quartz and K-feldspar produced little fine-grained material in the silty size fraction and was likely preserved in the coarser fractions (Minami *et al.*, 2017). The concentrations of heavy metals, such as Cu, Zn, Cd, Sn, and Pb, increased dramatically in fractions smaller than

Geochemical mapping of remote islands around Kyushu, Japan (Ohta)

Table 5 continued.

Table with columns: Element, Unit, Hr04#, Hr05, Hr06, Hr07, Hr08, Hr09, Os01, Os02, Mf01, Ik0102, Ik0103, Ik0104, Ik0105, Ik0106, Ik0107, Uk01, Uk02, Uk03, Oj01, Oj02, Nk01, Nk02, Nk03, Nk04, Nk05, Nk06, Nk07, Nk08, Nk09, Nk10, Nk11, Nk12. Rows list elements from Na2O to U. Values are in mg/kg or wt%.

* - The mean values of repeated analyses (n=3).

Geochemical mapping of remote islands around Kyushu, Japan (Ohta)

Table 5 continued.

Table with 42 columns (Element, Unit, Am09, Am10, Am11, Am12, Am13, Am14, Am15, Am16, Am17, Am18, Am19, Am20, Am21, Am22, Am23*, Am24, Am25, Am26, Am27, Am28, Am29, Am30, Am31, Am32, Am33, Am34, Am35, Am36, Am37, Am38, Am39, Am40, Am41) and rows for elements from Na2O to U.

* The mean values of repeated analyses (n=3).

Geochemical mapping of remote islands around Kyushu, Japan (Ohta)

Table 5 continued.

Element	Unit	Tn23	Tn24	Tn25	Tn26	Tn27	SK01	SK02	SK03	YK01 ^a	YK02	YK03	YK04	YK05	YK06	YK07	YK08	YK09	YK10	YK11	YK12	YK13	YK14	YK15	YK16	YK17	YK18	YK19	YK20	YK21	YK22	YK23	
Na ₂ O	wt%	1.23	1.53	1.23	1.03	1.02	3.04	2.78	2.95	3.43	3.90	4.06	0.934	0.757	1.06	1.78	2.80	3.56	3.36	2.23	3.00	2.68	4.34	3.93	3.43	3.27	3.67	4.09	3.63	3.54	3.05	3.20	
MgO	wt%	1.28	0.577	0.612	0.527	0.880	3.28	4.76	3.57	1.00	1.09	0.864	1.42	1.53	1.39	1.25	0.958	0.834	0.882	1.34	1.68	0.897	0.801	0.929	0.933	1.34	0.866	0.809	0.765	0.728	0.967	1.08	
Al ₂ O ₃	wt%	12.38	7.58	6.84	6.70	10.29	16.93	15.51	16.88	14.95	17.20	18.96	13.75	11.99	12.19	14.37	16.03	16.67	15.53	15.36	17.91	14.35	18.49	17.44	17.51	16.95	14.99	17.39	17.44	17.56	16.95	15.63	16.05
P ₂ O ₅	wt%	0.114	0.034	0.050	0.036	0.128	0.153	0.139	0.108	0.108	0.132	0.150	0.101	0.102	0.110	0.128	0.142	0.182	0.179	0.159	0.185	0.195	0.191	0.161	0.154	0.247	0.181	0.216	0.147	0.145	0.136	0.155	
K ₂ O	wt%	2.09	1.77	1.62	1.54	1.47	1.36	1.21	1.30	3.09	3.24	3.36	1.98	1.91	2.30	2.67	3.42	3.45	3.23	2.90	3.57	3.25	3.15	3.27	3.41	3.05	3.10	2.78	3.05	2.85	3.42	3.18	
CaO	wt%	0.634	0.273	0.237	0.222	0.658	7.30	7.46	7.33	2.55	2.87	2.88	0.757	0.743	0.904	1.32	1.99	2.39	2.34	1.92	2.31	1.71	1.81	2.92	2.73	2.40	2.66	3.04	2.43	2.53	2.16	2.37	
TiO ₂	wt%	0.885	0.387	0.484	0.851	0.581	0.776	0.981	0.820	0.452	0.582	0.532	0.741	0.838	0.757	0.629	0.564	0.492	0.499	0.781	1.06	0.481	0.478	0.472	0.490	1.05	0.548	0.453	0.498	0.462	0.551	0.633	
MnO	wt%	0.139	0.027	0.035	0.035	0.070	0.150	0.158	0.058	0.074	0.078	0.081	0.104	0.082	0.090	0.072	0.065	0.066	0.088	0.114	0.069	0.070	0.068	0.070	0.102	0.102	0.070	0.056	0.061	0.062	0.069	0.075	
T-Fe ₂ O ₃	wt%	5.34	2.01	2.47	2.99	3.74	7.68	10.3	8.25	2.58	3.16	3.43	5.24	5.27	4.49	4.66	3.39	3.03	2.75	4.94	5.00	2.75	2.93	2.99	2.96	3.76	3.04	2.44	3.04	2.90	3.13	3.26	
H ₂ O ⁻	wt%	2.03	0.852	0.653	0.755	2.84	0.398	0.986	0.200	0.65	0.607	0.934	2.42	1.95	1.93	2.12	0.798	0.695	0.462	2.38	1.20	0.715	0.684	0.800	0.779	0.559	0.469	0.458	0.607	1.25	0.655	0.580	
Li	mg/kg	37.9	30.8	24.8	24.9	28.0	17.3	16.1	17.0	37.1	43.2	62.8	42.7	41.4	46.0	49.1	55.3	62.8	49.3	43.3	79.2	49.5	61.6	51.2	45.6	35.2	46.9	40.6	48.4	41.7	43.3	39.4	
Be	mg/kg	1.69	0.897	0.95	0.93	1.09	1.15	1.03	1.05	3.93	4.94	5.7	1.90	2.31	2.54	3.47	4.56	5.24	4.30	3.39	4.97	2.94	6.00	5.37	4.67	4.42	4.93	5.12	5.13	4.86	4.33	4.30	
Sc	mg/kg	11.6	4.15	4.87	5.35	9.13	34.9	29.1	6.89	7.58	5.98	11.3	9.95	8.69	8.05	6.63	5.59	4.93	11.6	12.6	4.80	4.83	5.67	6.20	9.78	6.83	6.10	6.18	6.04	7.02	8.14		
V	mg/kg	105	39.1	42.4	51.8	67.4	181	285	201	28.3	32.9	84.0	78.1	73.3	66.9	42.3	27.5	30.8	79.8	49.9	30.9	32.1	34.4	43.6	35.9	24.4	30.7	36.7	36.5	32.0			
Cr	mg/kg	52.2	19.9	21.4	24.4	30.0	12.2	19.9	13.6	7.98	16.8	14.3	58.1	51.0	42.1	35.9	18.4	13.1	11.3	27.0	18.6	9.8	13.0	11.1	13.3	10.1	11.0	10.6	15.7	13.6	16.2	12.2	
Co	mg/kg	12.7	4.03	6.20	5.73	7.97	17.5	24.2	19.4	4.64	5.81	6.07	12.1	12.1	9.2	9.41	6.75	6.00	5.37	9.46	9.30	5.22	5.16	5.64	5.96	7.21	5.79	4.70	5.61	6.03	5.98	5.94	
Ni	mg/kg	22.2	7.96	9.40	9.66	14.1	4.98	6.65	5.44	3.90	7.82	7.28	25.1	24.3	19.8	17.4	8.71	6.86	5.20	13.3	9.11	5.42	6.49	5.86	6.48	4.96	5.53	5.15	7.46	6.74	7.39	6.20	
Cu	mg/kg	29.3	4.73	5.91	6.71	17.1	16.8	14.3	19.2	5.73	7.22	10.1	25.6	26.8	19.4	18.3	12.0	9.55	7.09	18.5	12.0	7.21	8.97	8.46	9.39	7.47	9.38	7.79	9.64	9.25	9.86	8.15	
Zn	mg/kg	138	41.4	50.8	43.7	70.3	94.2	102	88.0	40.3	59.1	86.8	131	126	90.7	89.5	67.8	66.6	62.3	97.1	82.6	50.0	83.6	55.9	56.8	56.9	48.8	41.2	57.3	47.0	58.1	55.6	
Ga	mg/kg	14.9	7.33	6.60	6.95	11.1	17.6	17.0	17.7	19.3	25.9	24.5	17.0	15.3	17.1	19.2	24.3	23.2	25.8	20.9	31.7	25.0	25.2	23.6	40.4	29.4	31.0	28.3	26.2	25.9	28.9		
As	mg/kg	6.64	4.83	5.03	5.03	6.48	4.18	3.33	4.54	9.41	5.17	13.8	24.9	31.6	41.7	18.8	15.1	17.8	14.9	16.7	18.2	15.8	23.2	11.9	6.41	15.1	13.3	9.42	4.54	8.09	20.9	17.2	
Rb	mg/kg	89.9	59.2	54.4	55.2	58.2	48.7	42.2	47.2	11.6	13.7	16.3	88.7	82.8	100	123	153	159	136	120	18.2	13.4	15.8	15.2	15.2	12.1	13.6	12.3	13.8	12.5	14.6	13.1	
Sr	mg/kg	10.1	81.7	71.3	76.9	278	26.2	27.9	15.2	16.8	17.4	72.6	72.1	76.2	120	133	152	152	126	137	137	137	171	171	158	146	162	181	156	163	144	140	
Y	mg/kg	14.3	7.56	8.21	7.90	14.9	24.7	23.8	24.7	18.3	29.9	24.0	12.3	11.6	13.2	13.1	24.0	29.7	32.3	19.4	41.3	36.0	28.4	27.4	25.0	70.8	34.9	39.5	26.9	25.0	28.0	36.6	
Zr	mg/kg	7.2	4.4	5.2	7.3	10.6	9.6	10.5	9.0	9.3	7.9	5.3	2.9	2.2	2.5	2.5	9.9	5.8	7.0	4.2	14	7.3	7.2	7.2	8.2	8.2	8.6	6.6	18	15	8.6	18	
Nb	mg/kg	11.8	6.74	8.23	10.8	8.67	4.98	4.62	4.83	7.45	10.5	14.6	11.9	12.1	11.2	12.9	14.2	10.6	11.1	21.2	11.9	14.7	12.3	13.5	12.4	11.6	13.0	11.9	11.5	11.5	11.5		
Mo	mg/kg	0.634	0.202	0.260	0.291	0.610	0.676	0.624	0.735	0.680	0.170	0.304	1.38	0.821	0.563	0.683	0.346	0.292	0.086	0.841	0.292	0.084	0.269	0.065	0.190	0.174	0.220	0.046	0.023	0.512	0.430	0.319	
Cd	mg/kg	0.154	0.038	0.058	0.056	0.124	0.136	0.141	0.134	0.055	0.087	0.104	0.212	0.511	0.236	0.359	0.118	0.096	0.094	0.250	0.152	0.124	0.150	0.119	0.078	0.081	0.072	0.079	0.139	0.075	0.106		
Sn	mg/kg	6.658	0.335	0.408	0.594	0.408	0.312	0.586	0.926	0.806	0.608	0.363	0.298	0.272	0.563	0.385	0.388	0.667	0.210	0.195	0.157	0.156	0.275	0.281	0.319	0.310	0.310	0.327	0.367	0.465			
Sb	mg/kg	6.00	2.20	2.14	2.19	3.06	2.87	2.50	2.84	8.52	12.0	17.3	9.43	10.2	10.4	13.0	15.3	17.1	11.1	8.85	18.8	9.66	15.0	12.7	11.1	8.48	12.7	11.2	13.3	12.0	12.1	10.5	
Cs	mg/kg	486	362	363	458	407	244	215	236	251	259	312	419	42.1	393	336	332	317	307	383	313	349	271	280	316	267	270	233	277	258	332	274	
La	mg/kg	21.7	17.3	17.0	15.8	18.3	13.9	12.2	13.6	66.8	124	68.0	21.7	26.7	56.4	33.7	97.4	111	164	61.0	188	180	177.7	106	86.6	685	153	167	119	102	126	174	
Ce	mg/kg	45.9	34.6	33.6	31.7	37.4	30.4	26.8	29.7	142	424	146	53.7	55.0	121	74.3	210	238	566	131	662	619	165	227	184	1430	326	356	255	218	267	255	
Pr	mg/kg	5.24	3.79	3.72	3.50	4.28	3.72	3.36	3.62	15.6	28.6	15.9	5.16	6.19	13.3	8.11	23.4	26.4	38.1	14.4	44.6	41.5	18.3	25.3	20.2	97.2	35.7	39.1	28.2	23.8	29.4	40.7	
Nd	mg/kg	18.9	13.8	13.1	12.4	16.4	15.4	14.0	15.1	57.1	104	57.6	19.0	22.8	48.7	29.9	84.8	96.7	138	52.6	162	150	66.5	92.6	74.2	355	130	144	103	87.1	106	148	
Sm	mg/kg	3.68	2.33	2.42	2.22	3.18	3.82	3.55	3.74	10.4	18.6	10.9	3.94	4.20	9.00	5.75	15.1	17.5															

Table 6 Element concentrations in stream sediments grouped into 7 grain size categories.

Element	Unit	SK03													In09													In26												
		B	C	D	E	F	G	A	B	C	D	E	F	G	A	B	C	D	E	F	G	A	B	C	D	E	F	G	A	B	C	D	E	F	G					
Na2O	wt%	3.19	3.01	2.93	3.03	3.07	3.08	1.43	2.23	1.54	0.913	1.13	1.37	1.28	1.30	1.56	1.09	0.773	1.23	1.67	1.44	1.34	1.31	1.06	0.866	1.08	1.72	1.94	1.44	1.34	1.31	1.06	0.866	1.08	1.72	1.94				
MgO	wt%	3.06	3.89	4.22	3.60	3.07	2.46	1.32	1.11	1.47	0.988	0.894	1.11	1.32	1.23	1.63	3.49	1.51	0.992	1.08	1.45	0.753	0.758	0.683	0.487	0.583	0.655	0.871	1.45	0.753	0.758	0.683	0.487	0.583	0.655	0.871				
Al2O3	wt%	16.35	15.97	15.97	16.98	17.46	16.83	14.36	17.67	11.93	7.80	10.68	14.64	17.30	12.89	13.78	8.98	7.09	9.77	12.72	16.60	0.969	10.19	7.98	6.00	7.28	9.86	12.68	9.69	10.19	7.98	6.00	7.28	9.86	12.68					
P2O5	wt%	0.171	0.158	0.150	0.152	0.154	0.169	0.112	0.098	0.066	0.048	0.075	0.125	0.159	0.099	0.086	0.062	0.047	0.066	0.093	0.136	0.116	0.099	0.046	0.028	0.043	0.063	0.082	0.116	0.099	0.046	0.028	0.043	0.063	0.082					
K2O	wt%	1.54	1.41	1.32	1.34	1.34	1.36	2.54	1.93	1.38	1.47	1.89	2.23	2.50	2.51	2.10	1.31	2.20	2.08	2.38	2.79	1.65	1.76	1.55	1.35	1.57	1.97	2.18	1.65	1.76	1.55	1.35	1.57	1.97	2.18					
CaO	wt%	6.73	6.97	7.24	7.50	7.53	7.13	1.09	3.57	2.60	0.848	0.547	0.489	0.804	0.630	5.07	1.06	1.24	0.733	0.640	0.803	0.426	0.399	0.309	0.443	2.05	0.526	0.667	0.426	0.399	0.309	0.443	2.05	0.526	0.667					
TiO2	wt%	0.808	0.824	0.848	0.823	0.780	0.778	0.576	0.469	0.451	0.579	0.757	0.762	0.804	0.607	0.507	0.173	0.100	0.056	0.065	0.092	0.026	0.034	0.031	0.024	0.078	0.029	0.046	0.026	0.034	0.031	0.024	0.078	0.029	0.046					
MnO	wt%	0.149	0.170	0.178	0.159	0.142	0.124	6.07	4.83	4.12	3.72	4.59	5.16	5.99	0.667	0.076	0.173	0.100	0.056	0.065	0.092	0.026	0.034	0.031	0.024	0.078	0.029	0.046	0.026	0.034	0.031	0.024	0.078	0.029	0.046					
T-Fe2O3	wt%	7.59	8.46	9.05	8.31	7.69	7.43	6.07	4.83	4.12	3.72	4.59	5.16	5.99	5.89	5.39	9.71	8.19	4.12	4.08	5.43	7.06	6.34	3.40	2.51	7.85	3.43	4.45	7.06	6.34	3.40	2.51	7.85	3.43	4.45					
H2O-	wt%	0.099	0.098	0.294	0.199	0.200	0.589	2.27	1.80	1.24	0.865	1.65	3.82	4.53	1.65	1.36	0.727	0.679	1.16	2.14	3.09	1.32	1.22	0.873	0.671	0.637	1.08	1.49	1.32	1.22	0.873	0.671	0.637	1.08	1.49					
Li	mg/kg	17.6	17.0	16.6	16.9	17.1	17.5	43.1	33.9	25.7	23.3	31.0	39.3	44.5	44.5	39.2	24.4	22.6	29.0	35.8	45.3	43.6	41.5	30.4	22.7	24.9	33.2	40.8	43.6	41.5	30.4	22.7	24.9	33.2	40.8					
Be	mg/kg	1.14	1.12	1.04	1.08	1.10	1.10	2.10	1.84	1.18	0.928	1.37	1.85	2.25	2.02	1.79	1.10	1.02	1.30	1.74	2.30	1.66	1.60	1.07	0.787	1.11	1.46	1.81	1.66	1.60	1.07	0.787	1.11	1.46	1.81					
Sc	mg/kg	26.6	29.7	31.4	28.5	26.5	23.5	9.95	9.43	10.92	7.22	8.21	11.0	13.8	8.96	11.0	21.0	10.5	7.05	8.01	12.8	5.57	6.08	4.86	3.66	8.47	5.19	7.90	5.57	6.08	4.86	3.66	8.47	5.19	7.90					
V	mg/kg	173	197	224	201	188	177	80.4	64.8	56.8	65.9	90.5	90.5	101	87.3	73.3	192	204	92.7	72.9	93.2	54.1	54.5	40.2	37.9	185	51.0	61.1	54.1	54.5	40.2	37.9	185	51.0	61.1					
Cr	mg/kg	10.3	13.0	14.6	14.0	12.8	12.4	56.8	42.8	26.6	23.2	35.2	48.0	64.7	58.2	49.4	37.4	34.7	41.9	52.7	73.9	41.0	36.7	22.8	17.3	37.5	34.7	50.5	41.0	36.7	22.8	17.3	37.5	34.7	50.5					
Co	mg/kg	17.1	19.3	21.1	18.9	17.1	15.6	9.89	8.78	8.95	7.47	9.45	11.8	14.9	9.04	9.58	18.2	14.0	8.45	8.94	12.0	10.0	9.87	6.35	4.77	11.0	7.67	11.6	10.0	9.87	6.35	4.77	11.0	7.67	11.6					
Ni	mg/kg	4.66	5.22	5.76	5.36	4.86	5.56	24.3	18.4	12.9	10.3	15.4	20.9	27.7	25.1	21.1	14.2	14.1	18.7	23.0	31.7	22.3	20.3	11.9	8.02	11.7	15.3	22.5	22.3	20.3	11.9	8.02	11.7	15.3	22.5	22.3				
Cu	mg/kg	17.3	17.6	16.9	17.4	19.2	28.6	24.0	18.2	11.3	8.3	12.8	19.5	26.4	21.2	17.1	10.6	9.8	12.2	16.8	24.8	16.2	14.7	8.49	5.20	8.36	11.4	15.5	16.2	14.7	8.49	5.20	8.36	11.4	15.5					
Zn	mg/kg	85.5	89.2	92.0	85.4	81.1	79.0	80.3	66.7	58.2	48.9	64.3	80.0	96.1	71.3	70.4	110	94.5	62.6	74.1	97.3	77.0	76.9	48.7	36.1	93.8	60.7	74.2	76.9	48.7	36.1	93.8	60.7	74.2						
As	mg/kg	3.86	3.54	3.88	4.24	4.92	7.96	10.2	7.66	5.85	3.95	5.41	8.16	10.2	14.8	8.84	4.69	3.84	4.90	6.47	9.81	15.9	15.3	7.57	4.10	5.58	7.89	10.5	15.9	15.3	7.57	4.10	5.58	7.89	10.5					
Rb	mg/kg	55.3	50.3	46.9	47.2	47.8	46.2	113	84.0	54.7	53.8	73.9	94.0	116	106	88.7	50.5	54.4	79.0	96.7	128	70.7	72.1	58.9	47.1	55.9	75.5	92.4	70.7	72.1	58.9	47.1	55.9	75.5	92.4					
Sr	mg/kg	263	259	262	280	289	284	117	236	164	81.2	84.0	95.0	94.8	86.4	143	107	65.3	84.1	97.4	98.8	82.7	92.0	82.0	66.9	75.5	96.3	111	82.7	92.0	82.0	66.9	75.5	96.3	111					
Y	mg/kg	27.3	26.2	25.0	24.8	24.6	23.5	15.1	12.7	9.69	7.60	12.2	21.3	25.1	13.6	11.8	10.1	7.66	10.5	13.9	21.2	11.92	11.5	7.47	5.59	9.77	12.0	15.6	11.92	11.5	7.47	5.59	9.77	12.0	15.6					
Zr	mg/kg	121	111	103	103	104	106	77	60	42	37	65	117	132	89	58	36	36	60	84	107	45	43	32	25	72	69	79	45	43	32	25	72	69	79					
Nb	mg/kg	5.59	5.13	4.73	4.83	4.82	5.14	11.0	8.63	5.74	6.57	9.72	12.5	14.4	11.2	9.07	6.13	7.40	9.95	11.6	14.9	8.42	7.59	5.38	6.03	19.6	10.3	13.4	8.42	7.59	5.38	6.03	19.6	10.3	13.4					
Mo	mg/kg	0.790	0.656	0.647	0.702	0.700	0.993	0.710	0.631	0.459	0.298	0.479	0.732	1.04	0.814	0.610	0.400	0.372	0.448	0.555	0.956	0.793	0.866	0.488	0.233	0.669	0.470	0.767	0.793	0.866	0.488	0.233	0.669	0.470	0.767					
Cd	mg/kg	0.127	0.116	0.121	0.123	0.119	0.129	0.099	0.102	0.081	0.058	0.094	0.146	0.177	0.113	0.105	0.101	0.078	0.100	0.138	0.179	0.069	0.073	0.049	0.037	0.058	0.069	0.096	0.069	0.073	0.049	0.037	0.058	0.069	0.096					
Sn	mg/kg	1.41	1.36	1.30	1.37	1.33	1.73	2.08	1.65	1.14	0.993	1.62	2.19	3.23	2.09	1.64	1.17	1.25	1.45	1.93	3.41	1.30	1.30	0.980	0.735	1.85	1.73	2.36	1.30	1.30	0.980	0.735	1.85	1.73	2.36					
Sb	mg/kg	0.360	0.275	0.254	0.245	0.254	0.364	0.840	0.751	0.469	0.430	0.527	0.918	0.870	0.708	0.421	0.389	0.596	0.618	0.793	0.832	0.779	0.611	0.379	0.539	0.624	0.739	0.779	0.611	0.379	0.539	0.624	0.739							
Cs	mg/kg	3.28	3.01	2.87	2.86	2.93	2.72	6.97	5.27	3.08	2.34	3.69	5.52	7.54	5.90	5.04	2.64	2.64	3.51	4.98	8.04	3.69	3.78	2.71	1.84	2.37	3.46	5.12	3.69	3.78	2.71	1.84	2.37	3.46	5.12					
Ba	mg/kg	270	248	229	235	238	251	422	329	287	320	405	434	452	480	410	278	355	497	537	562	355	356	342	356	498	535	600	355	356	342	356	498	535	600					
La	mg/kg	15.2	14.1	13.4	13.6	13.6	13.8	27.0	20.7	14.0	13.9	19.5	36.0	36.2	28.9	21.6	12.3	14.2	24.6	28.8	38.1	19.9	18.5	13.3	11.7	26.5	31.4	30.3	19.9	18.5	13.3	11.7	26.5	31.4	30.3					
Ce	mg/kg	33.7	31.1	29.3	29.7	30.1	29.5	52.6	40.4	28.0	27.0	39.0	73.5	75.7	57.1	42.3	24.3	27.8	52.4	59.9	75.9	40.6	37.6	26.3	22.7	52.9	65.6	63.2	40.6	37.6	26.3	22.7	52.9	65.6	63.2					
Pr	mg/kg	4.18	3.85	3.64	3.66	3.68	3.70	6.26	4.66	3.23	3.17	4.52	8.35	8.51	6.46	4.79	2.89	3.30	6.22	6.81	8.81	4.68	4.33	3.03	2.57	6.08	7.43	7.04	4.68	4.33	3.03	2.57	6.08	7.43	7.04					
Nd	mg/kg	17.1	16.0	15.0	15.2	15.1	15.3	22.4	17.0	11.8	11.3	16.6	30.5	31.2	22.9	17.4	10.9	12.1	23.0	24.9	32.1	17.5	16.4	11.0	9.56	21.5	26.9	25.6	17.5	16.4	11.0	9.56	21.5	26.9	25.6					
Sm	mg/kg	4.01	3.86	3.66	3.63	3.67	3.55	4.10	2.98	2.27	2.05	3.07	5.68	5.85	3.86	3.06	2.17	2.12	4.06	4.36	5.74	3.28	3.13	2.11	1.71	3.88	4.93	4.82	3.28	3.13	2.11	1.71	3.88	4.93	4.82					
Eu	mg/kg	1.07	1.01	1.01	1.02	1.05	1.02	0.844	0.939	0.692	0.473	0.659	0.981	1.19	0.755	0.798	0.570	0.471	0.804	0.778	1.13	0.721</																		

Table 6 continued.

Element	Unit	Yk01							Yk17					
		A	B	C	D	E	F	G	A	B	C	D	E	F+G
Na ₂ O	wt%	1.13	1.54	2.44	3.14	3.48	3.41	2.80	1.20	1.49	1.97	2.35	3.27	3.33
MgO	wt%	0.987	1.15	1.10	1.04	0.965	1.01	1.25	0.896	1.05	2.49	2.58	1.10	0.816
Al ₂ O ₃	wt%	9.67	11.73	13.82	14.08	14.91	16.77	18.49	9.38	10.54	10.93	11.27	14.82	18.11
P ₂ O ₅	wt%	0.053	0.048	0.045	0.057	0.142	0.271	0.196	0.056	0.049	0.054	0.106	0.282	0.214
K ₂ O	wt%	4.14	4.48	4.06	3.28	2.83	2.63	2.50	4.05	3.83	3.06	2.42	2.86	3.09
CaO	wt%	0.49	1.04	1.87	2.36	2.54	2.29	1.50	0.545	1.14	2.23	2.30	2.45	2.17
TiO ₂	wt%	0.577	0.601	0.478	0.503	0.761	0.922	0.902	0.507	0.469	1.00	2.63	1.67	0.94
MnO	wt%	0.063	0.069	0.064	0.060	0.070	0.084	0.075	0.058	0.064	0.141	0.204	0.119	0.091
T-Fe ₂ O ₃	wt%	3.90	4.13	3.49	3.41	4.18	5.00	5.27	3.33	3.34	8.05	17.2	8.34	4.42
H ₂ O ⁻	wt%	0.502	0.535	0.741	0.513	0.656	1.64	3.87	0.381	0.487	0.365	0.324	0.546	1.36
Li	mg/kg	95.4	97.4	67.5	40.7	34.9	53.2	73.2	79.2	70.8	47.9	30.0	34.1	48.0
Be	mg/kg	2.09	2.18	2.67	3.41	4.02	4.81	4.50	2.13	2.12	2.25	2.84	4.45	5.77
Sc	mg/kg	7.98	8.83	8.17	7.25	8.00	8.80	11.8	5.39	7.30	16.5	20.0	9.65	7.98
V	mg/kg	33.7	33.8	38.8	50.5	77.8	78.6	69.6	33.2	31.2	153	416	190	76.0
Cr	mg/kg	18.8	18.0	12.2	8.6	10.4	20.0	43.5	14.4	12.7	13.4	17.4	13.6	22.8
Co	mg/kg	5.86	6.42	5.64	5.65	6.90	7.64	8.98	5.20	5.65	13.6	24.7	11.8	8.21
Ni	mg/kg	6.93	7.17	5.18	3.94	4.89	8.95	18.2	5.80	5.93	5.76	6.30	5.57	10.4
Cu	mg/kg	6.62	6.49	5.04	4.42	6.39	13.9	24.5	4.98	5.32	5.49	7.68	6.94	15.0
Zn	mg/kg	67.8	73.0	57.7	46.5	61.2	83.1	107	59.8	58.1	94.8	176	101	101
Ga	mg/kg	13.9	16.1	16.3	16.1	23.4	41.5	29.7	13.0	13.1	14.7	24.4	50.4	31.4
As	mg/kg	7.86	6.49	6.42	6.63	9.09	20.5	32.8	6.59	8.63	5.71	7.37	13.8	22.4
Rb	mg/kg	195	211	176	128	113	120	134	185	176	130	93.5	113	151
Sr	mg/kg	70.4	94.7	132	145	148	145	122	71.0	90.4	110	115	148	156
Y	mg/kg	9.07	8.82	7.38	7.86	25.3	65.0	33.8	9.14	9.23	10.6	25.1	84.3	42.8
Zr	mg/kg	3.8	3.9	6.0	6.4	12	34	37	2.1	2.7	6.7	16	20	17
Nb	mg/kg	15.3	16.8	11.8	7.11	8.26	15.4	20.0	13.2	12.1	9.18	9.30	13.5	16.5
Mo	mg/kg	0.255	0.176	0.134	0.151	0.307	0.852	1.81	0.000	0.030	0.057	0.244	0.257	0.618
Cd	mg/kg	0.021	0.038	0.042	0.053	0.075	0.084	0.090	0.032	0.036	0.062	0.078	0.090	0.137
Sn	mg/kg	6.00	6.71	5.30	3.61	4.42	6.74	12.1	5.08	4.70	3.79	3.49	4.35	8.40
Sb	mg/kg	5.43	0.397	0.465	0.299	0.475	1.20	1.98	0.116	0.158	0.131	0.119	0.155	0.361
Cs	mg/kg	14.8	16.3	13.1	8.87	8.39	11.8	16.0	12.1	11.6	8.33	6.02	8.04	12.9
Ba	mg/kg	470	381	303	253	246	273	315	422	315	235	194	264	358
La	mg/kg	22.1	19.6	14.8	16.4	102	323	92.8	21.5	17.5	18.0	108	513	164
Ce	mg/kg	45.4	40.3	30.1	33.5	217	691	204	45.0	36.0	37.4	230	1086	351
Pr	mg/kg	5.17	4.62	3.36	3.70	23.6	75.8	22.1	5.15	4.12	4.28	25.1	119	38.8
Nd	mg/kg	19.2	17.1	12.4	13.7	87.1	278	82.2	18.9	15.2	15.8	92.9	438	142
Sm	mg/kg	3.74	3.36	2.39	2.68	15.5	49.8	15.8	3.63	3.08	3.08	16.1	74.5	25.5
Eu	mg/kg	0.487	0.573	0.752	0.840	0.997	1.34	1.24	0.484	0.517	0.627	0.768	1.43	1.28
Gd	mg/kg	2.76	2.53	1.93	2.17	11.1	34.1	11.3	2.81	2.36	2.58	11.1	49.7	17.6
Tb	mg/kg	0.350	0.319	0.259	0.274	1.19	3.56	1.43	0.354	0.316	0.329	1.22	5.17	2.06
Dy	mg/kg	1.81	1.73	1.36	1.49	5.73	16.2	7.64	1.85	1.71	1.96	5.69	21.8	9.62
Ho	mg/kg	0.302	0.301	0.251	0.277	0.910	2.35	1.24	0.310	0.307	0.363	0.893	3.07	1.50
Er	mg/kg	0.768	0.769	0.658	0.721	2.01	4.98	3.13	0.773	0.751	0.997	2.04	6.07	3.44
Tm	mg/kg	0.098	0.104	0.093	0.097	0.251	0.574	0.415	0.109	0.109	0.146	0.251	0.662	0.429
Yb	mg/kg	0.606	0.657	0.590	0.633	1.42	2.99	2.56	0.656	0.674	0.863	1.50	3.25	2.40
Lu	mg/kg	0.084	0.089	0.085	0.089	0.194	0.389	0.351	0.085	0.090	0.139	0.219	0.451	0.342
Hf	mg/kg	0.13	0.13	0.14	0.19	0.33	1.1	1.1	0.08	0.11	0.22	0.49	0.69	0.57
Ta	mg/kg	1.46	1.74	1.41	0.91	1.09	2.07	2.52	1.19	1.14	0.97	1.08	1.75	2.19
Hg	mg/kg	0.004	0.004	0.003	0.005	0.010	0.044	0.121	0.002	0.002	0.003	0.005	0.009	0.028
Tl	mg/kg	0.987	1.09	0.881	0.616	0.544	0.635	0.795	0.895	0.853	0.626	0.451	0.552	0.782
Pb	mg/kg	42.9	34.3	34.8	35.0	43.4	69.5	115	22.5	22.5	24.9	31.3	34.4	50.7
Bi	mg/kg	0.337	0.287	0.265	0.282	0.363	0.794	1.30	0.268	0.370	0.337	0.359	0.887	0.945
Th	mg/kg	8.97	7.64	5.17	5.87	41.8	141	37.7	8.95	6.75	6.01	44.2	215	67.7
U	mg/kg	1.74	1.72	1.48	1.44	3.25	9.77	9.74	1.52	1.39	1.37	3.05	14.7	7.71

A: 2-1 mm, B: 1-0.5 mm, C: 500-250 μ m, D: 250-125 μ m, E: 125-63 μ m, F: 63-32 μ m, G: <32 μ m

the coarse silt fraction (32–63 μ m), as with the Tn02, Tn09, and Tn26 samples. The concentrations of P₂O₅, Y, lanthanide (Ln: La–Lu), Th, and U were significantly high for Yk01 and Yk17 in the fine sand fractions of 63–250 μ m. The steep slope of the riverbed in Yakushima Island (3/100–1/50) (Shimazu and Nishi, 2004) and the high river discharge due to heavy rainfall (about 3,250–4,480 mm/year) (Meteorological Agency, <http://www.jma.go.jp/jma/menu/menureport.html>, accessed 2018-9-4) caused the accumulation of accessory minerals with a greater specific gravity than quartz, plagioclase, and K-feldspar in the fine sand fraction. Mafic elements, such as MgO, TiO₂, and Fe₂O₃ in Yk17, were very abundant in the fine sand fraction (125–250 μ m). Their systematic variations reflect

the relative abundance of magnetic minerals in clastics. Actually, the relative weight ratio of magnetic minerals removed using a hand magnet to the total <180 μ m fraction is extremely high in Yk12 (26%) and Yk17 (31%), but low for other samples (< 6%). The concentrations of mafic elements in the <180 μ m fraction were comparable to those for the coarse sand fraction (A, B, and C) and those for silty size fractions (F and G) (Tables 5 and 6). Thus, the procedure to remove excessive magnetic minerals from the fine sand fraction using a magnet was validated (Imai *et al.*, 2004).

Minami *et al.* (2017) reported that stream sediments derived from granitic rocks have variation patterns similar to that shown in Fig. 4: A V-shaped pattern and the

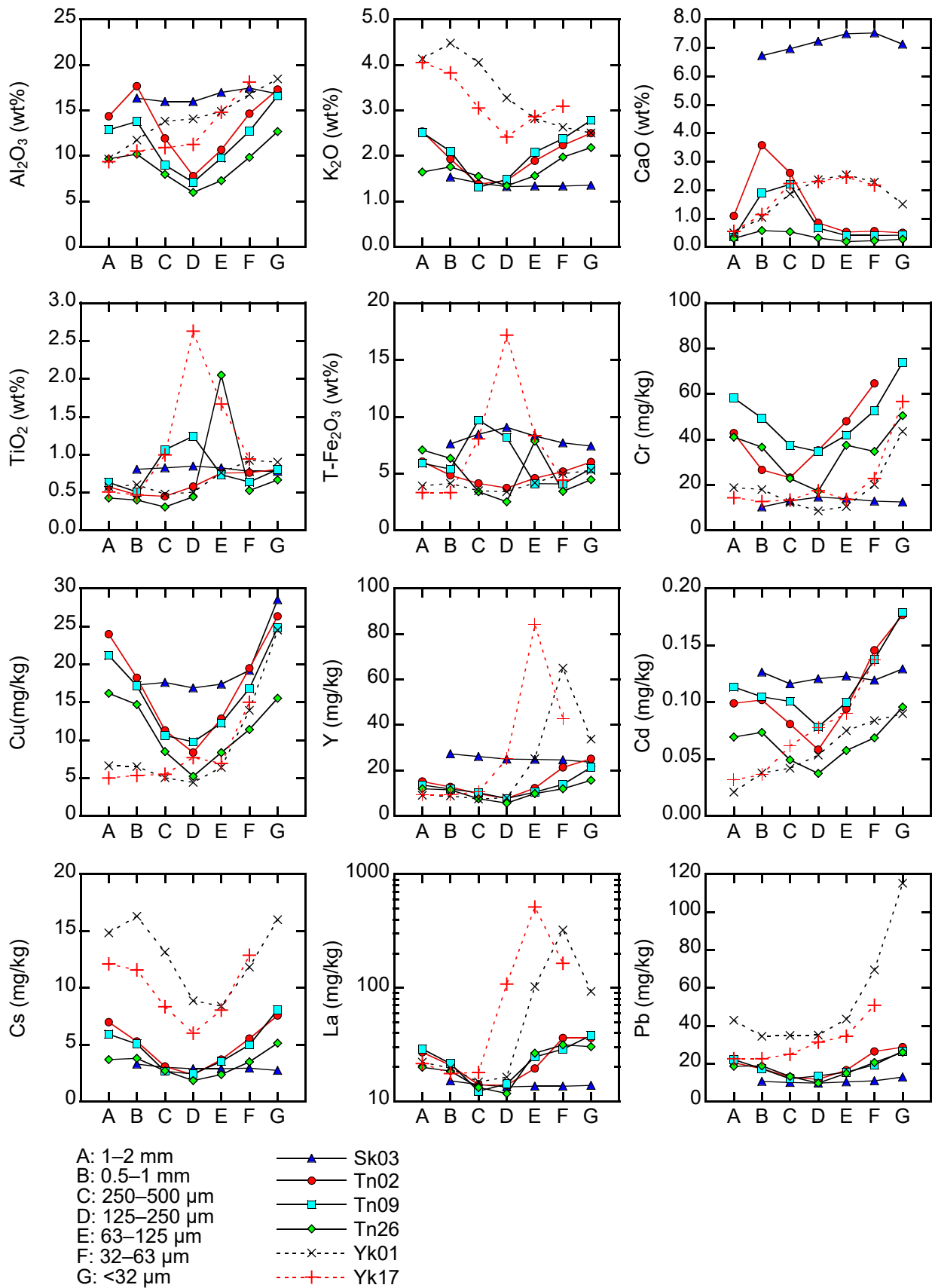


Fig. 4 Element concentrations in stream sediments by grain size category.

systematic decrease or increase in SiO₂, K₂O, CaO, Rb, Sr, and Ba concentrations. The element concentrations in the fine sand fraction (300–75 μm) of stream sediments were comparable to those of the host rocks. This is because quartz, K-feldspar, and plagioclase in stream sediments are more abundantly preserved in the coarse sand fraction (>300 μm) and finer grained accessory minerals have higher concentrations in the silty size fraction (<75 μm) than in the host rocks. Therefore, the fine sand fraction of <180 μm was less likely accumulate rock-forming minerals and was suitable for use in geochemical mapping.

4. 2 Element concentrations in fine stream sediments collected from remote islands around Kyushu

Figures 5–9 show geochemical maps for Al₂O₃, K₂O, CaO, T-Fe₂O₃, Cr, Zn, Nb, Cd, La, and Yb on remote islands around the Kyushu mainland. The maps were prepared using the ArcGIS 10.5 software. The geochemical maps were created following the method of Ohta *et al.* (2004). Element concentration intervals in the color image maps were categorized into 8 classes according to the percentile range: 0 ≤ x ≤ 5, 5 < x ≤ 10, 10 < x ≤ 25, 25 < x ≤ 50, 50 < x ≤ 75, 75 < x ≤ 90, 90 < x ≤ 95, and 95 < x ≤ 100%, where x represents the element concentration, according to Reimann (2005).

Enrichment with Li, Be, Na₂O, K₂O, CaO, Rb, Y, Nb, Sn, Cs, Ln, Ta, Tl, Pb, Th, and U was found in stream sediments collected from Yakushima Island, which is underlain mainly by Neogene granitic rock (Figs. 5–8). Stream sediments derived from Paleogene-Neogene sediment on Tsushima Island and stream sediments from Paleogene and Cretaceous sedimentary rocks on Amakusa Islands had abundant Li, Be, K₂O, Rb, Cs, La, Ce, Pr, Nd, Tl, and Th (Figs. 5 and 8). Stream sediments from Tanegashima Island had average chemical compositions for all samples but were poor in MgO, CaO, Sc, TiO₂, V, T-Fe₂O₃, Co, and Sr (Fig. 6). Islands with mafic volcanic and pyroclastic rocks outcrops, such as Ikinoshima, Hiradojima, Nagashima, and Sakurajima Islands, contained high amounts of Al₂O₃, MgO, CaO, P₂O₅, Sc, TiO₂, V, MnO, T-Fe₂O₃, Co, Cu, Zn, and Sr (Figs. 5 and 6). Their spatial distributions were influenced by the abundance of mafic minerals (olivine, pyroxene, and hornblende) in stream sediments. Stream sediments derived from alkaline mafic volcanic rocks on Ikinoshima, Ikitsushima, Takashima, Ukujima, and Ojikajima Islands were also highly enriched with Cr, Ni, Zn, Nb, Ln, and Ta. These elements are relatively uncommon in stream sediments derived from non-alkaline mafic volcanic and pyroclastic rocks distributed on Hiradojima, Nagashima, and Sakurajima Islands (Figs. 7 and 8). However, the reason for the lack of abundance of Na₂O and K₂O in stream sediments derived from alkaline mafic volcanic rocks is unclear because the host rock is enriched with Na₂O and K₂O.

The Cu, Zn, As, Mo, Cd, Sn, Sb, Hg, Pb, and Bi in stream sediments were influenced strongly by mineral

deposits. They were abundant in stream sediments from the south part of Tsushima Island, Ikinoshima Island, Ikitsushima Island, Takashima Island, Ukujima Island, and Ojikajima Island (Fig. 9). The Ts18 sample, in particular, had extremely high concentrations of Zn (1,855 mg/kg), Cd (16.6 mg/kg), and Pb (1,452 mg/kg) due to the Taishu Mine containing Zn and Pb in its drainage basin. The Am25 sample also had very high concentrations of Mo (51.4 mg/kg) and Sn (22.7 mg/kg) and rather high amounts of Cu (278 mg/kg), Zn (436 mg/kg), and Pb (222 mg/kg). However, no metalliferous mines or contaminant sources were found in the sampling location. In contrast, the Am42 and Am43 samples had the highest concentrations of Sb (1.41 mg/kg and 6.32 mg/kg, respectively) because of the Takahama Mine containing Sb located in the drainage basin of Am42 and near the sampling location of Am43. The W mines in the Yakushima Islands did not elevate concentrations of heavy metals in stream sediments. The high concentrations of Sn and Pb on Yakushima Island appear to be caused not by a W mine, but by the parent lithology (granitic rock).

4. 3 Abundance patterns for elements in stream sediments normalized to Japanese stream sediments

Figures 10 and 11 display median element concentrations for stream sediments normalized to the median concentrations of Japanese stream sediments (Imai *et al.*, 2004). Stream sediment samples were classified based on the dominant lithology in the watershed (Tables 2 and 3). Ikinoshima Island is mostly covered by both alkaline and non-alkaline mafic volcanic rock (Fig. 2c). The chemical compositions of sediments samples derived from alkaline mafic volcanic rock (a-Mv) and non-alkaline rock (Mv) were mutually consistent. Thus, Ikinoshima samples were classified as a mixture type of a-Mv and Mv (a-Mv+Mv). Similarly, stream sediment samples collected from Hiradojima Island were classified as a mixture of non-alkaline pyroclastic (Py) and mafic volcanic (Mv) rocks (Py+Mv) because these rock types are distributed together in the drainage basins (Table 3).

Geochemical abundance patterns for stream sediments derived from alkaline mafic volcanic rock (a-Mv) were similar among samples collected from the northern islands (Fig. 10a). Stream sediments were enriched with P₂O₅, TiO₂, Cr, MnO, T-Fe₂O₃, Co, Ni, Nb, La, Ce, Pr, Nd, Sm, and Ta, but were poor in Na₂O and CaO compared to Japanese stream sediments. In contrast, some differences were found in the geochemical abundance patterns for stream sediments from Hiradojima, Nagashima, and Sakurajima Islands, where non-alkaline mafic volcanic (Mv) and pyroclastic (Py) rock outcrops were present (Fig. 10b). In contrast with stream sediments derived from alkaline mafic volcanic rock (a-Mv), the abundance ratios relative to Japanese stream sediments were nearly constant among mafic elements (Sc, TiO₂, V, MnO, T-Fe₂O₃, and Co) and among Y and Ln. Volcanic ash deposits on Sakurajima Island were extremely poor in

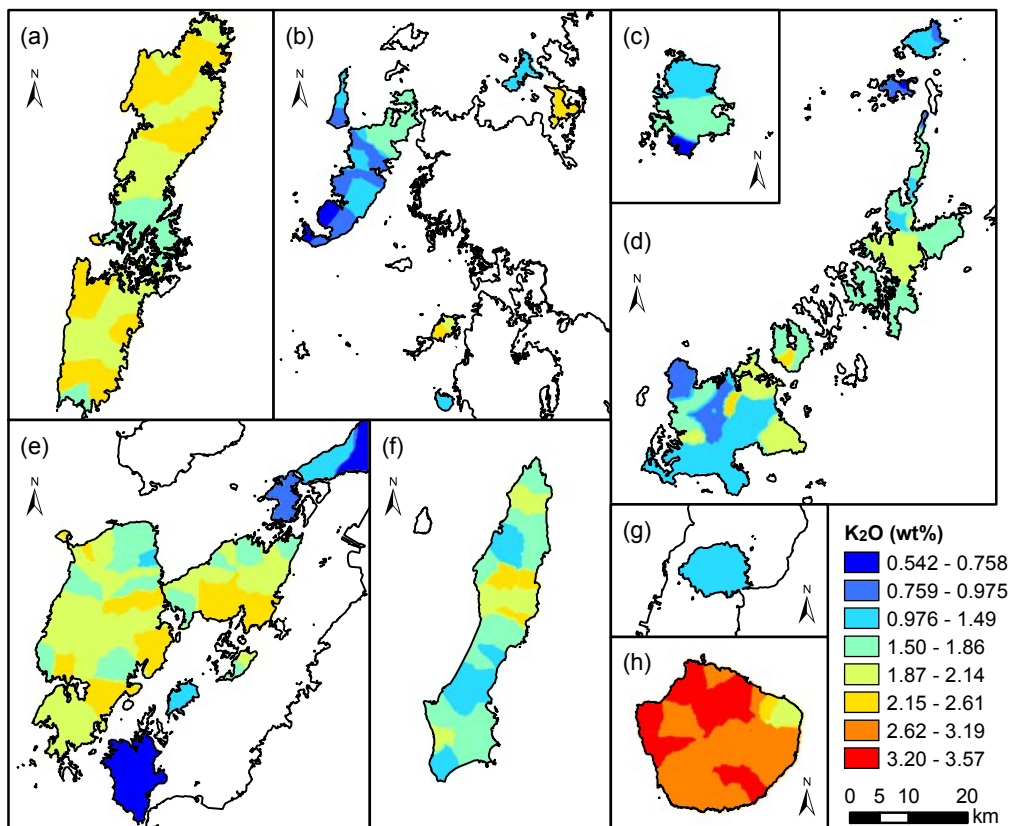
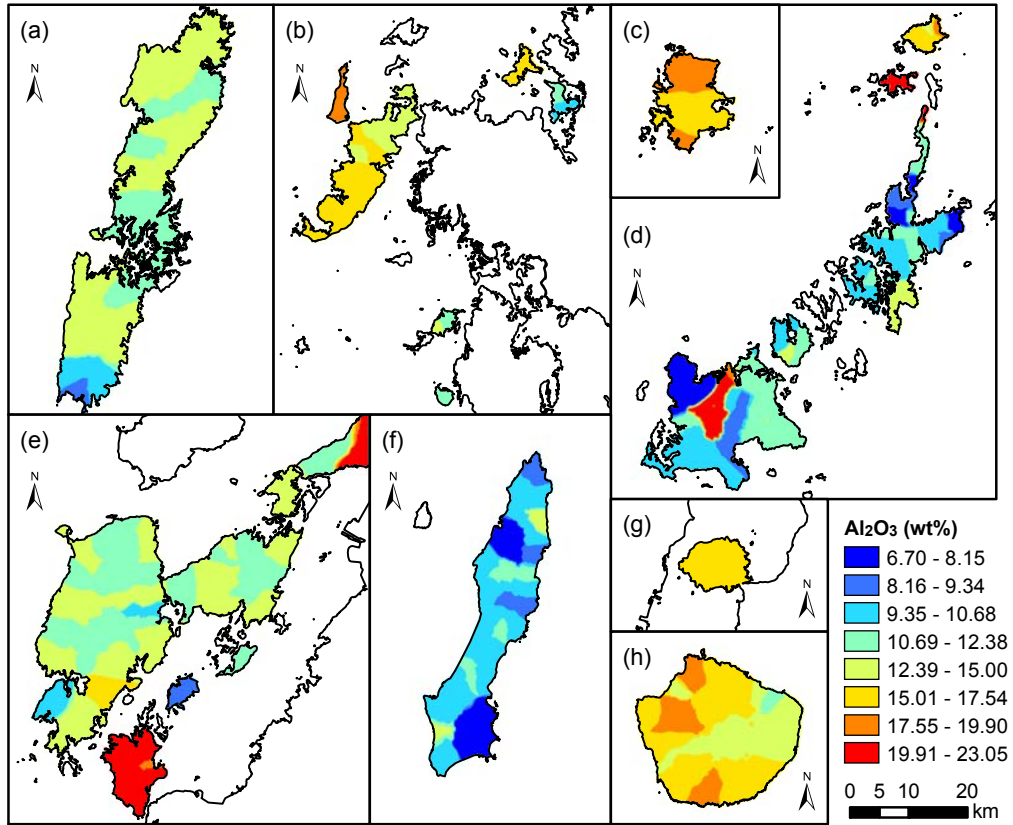


Fig. 5 Spatial distribution of Al₂O₃ and K₂O concentrations on remote islands. (a)-(h) are the same as Fig. 1.

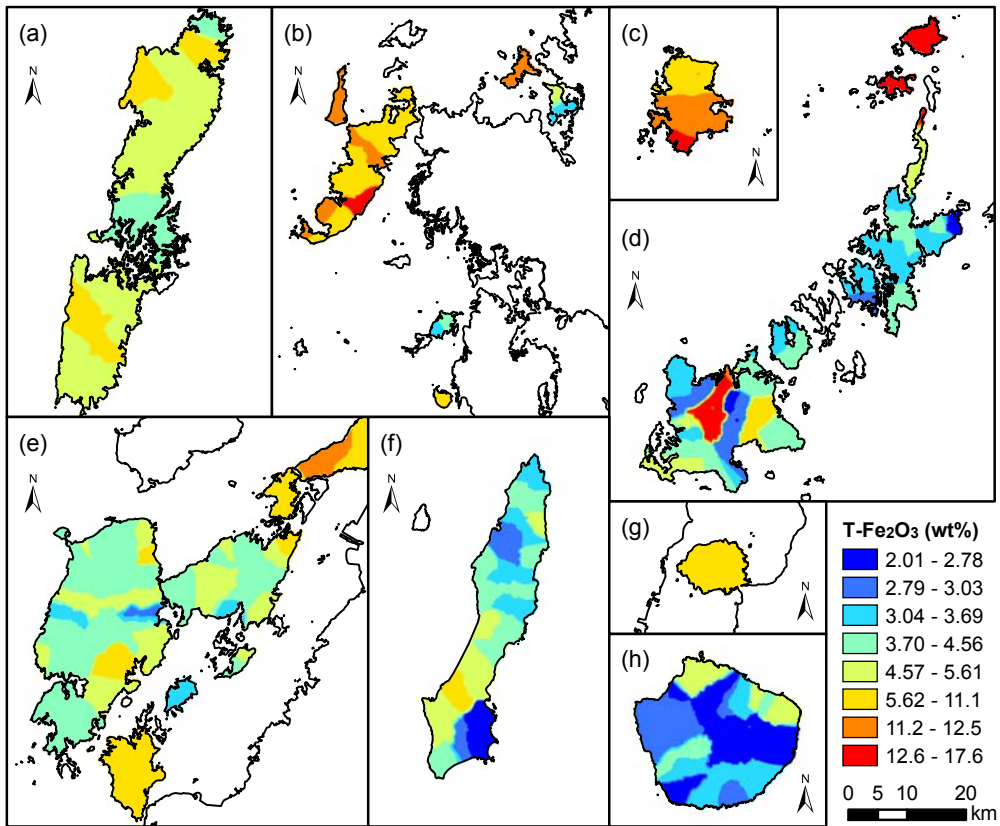
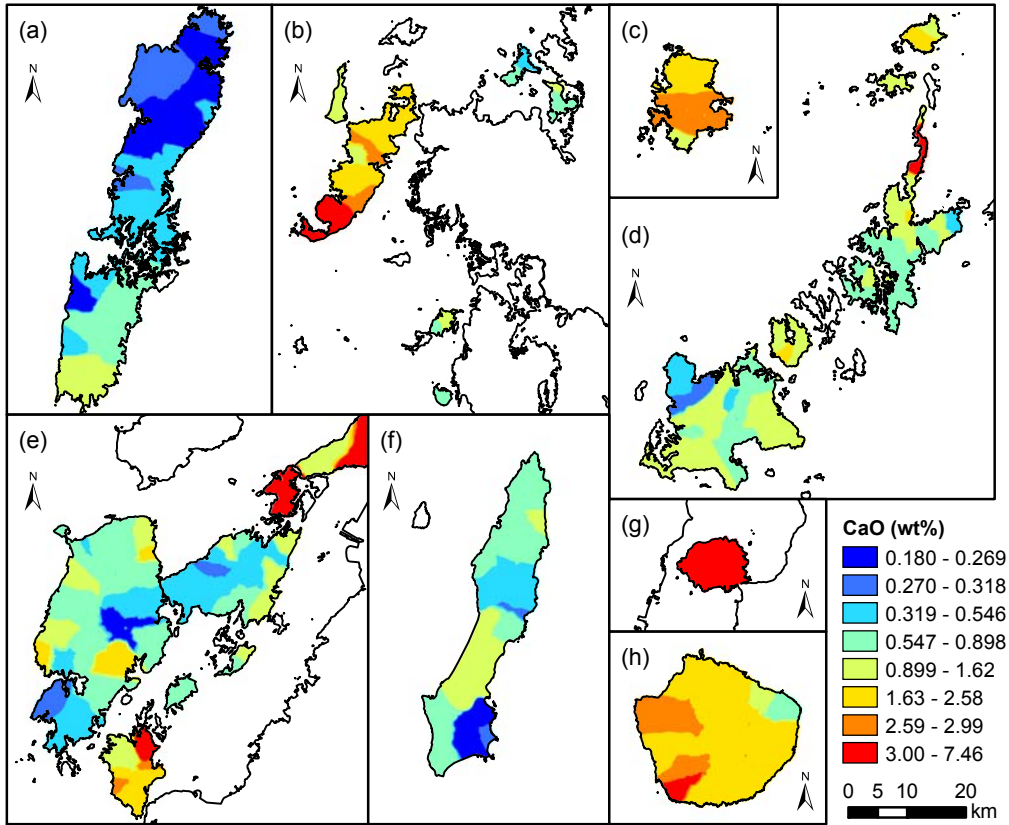


Fig. 6 Spatial distributions of CaO and T-Fe₂O₃ concentrations on remote islands. (a)-(h) are the same as Fig. 1.

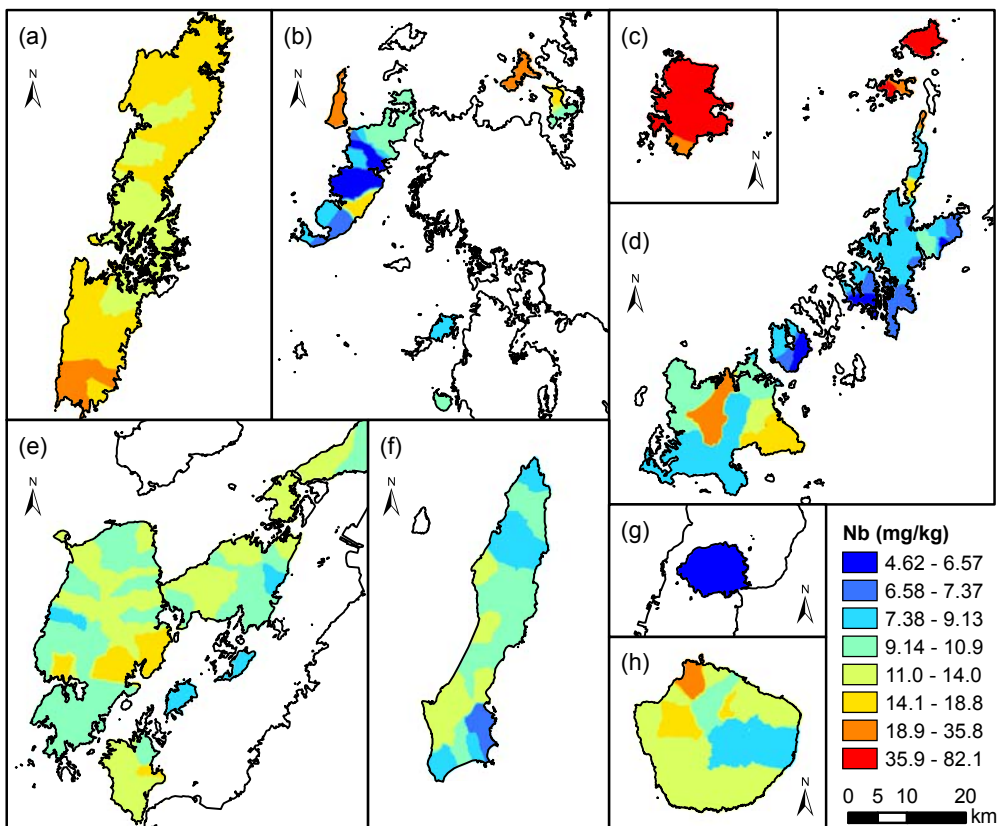
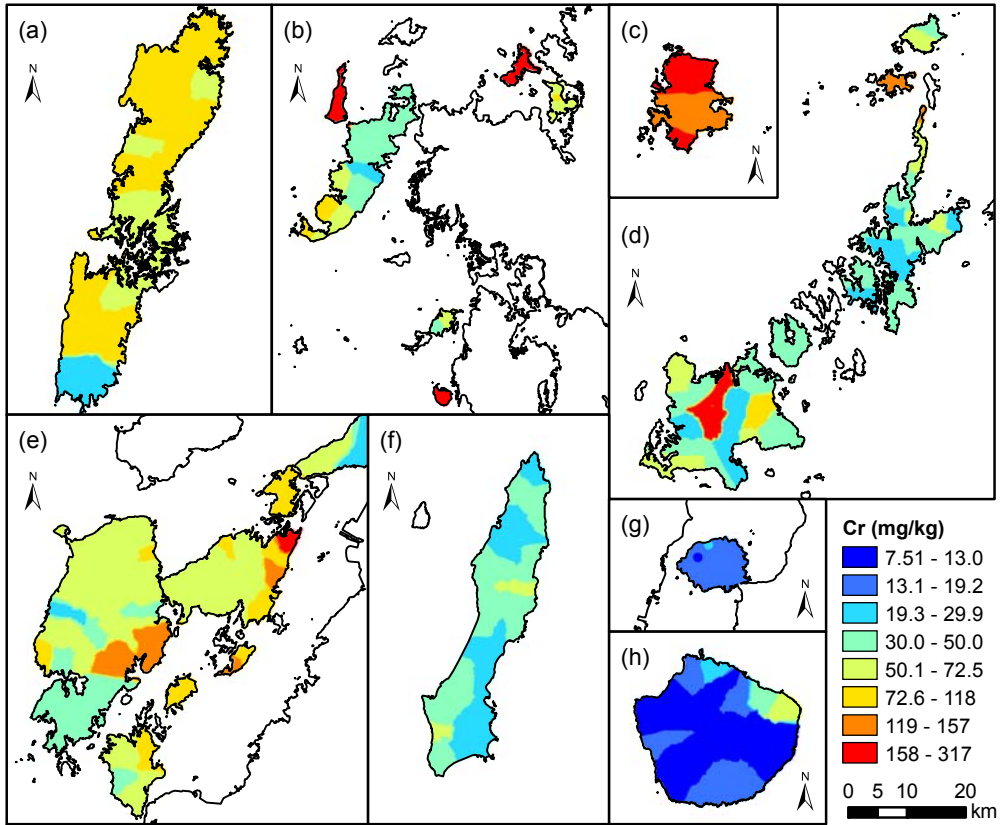


Fig. 7 Spatial distributions of Cr and Nb concentrations on remote islands. (a)-(h) are the same as Fig. 1.

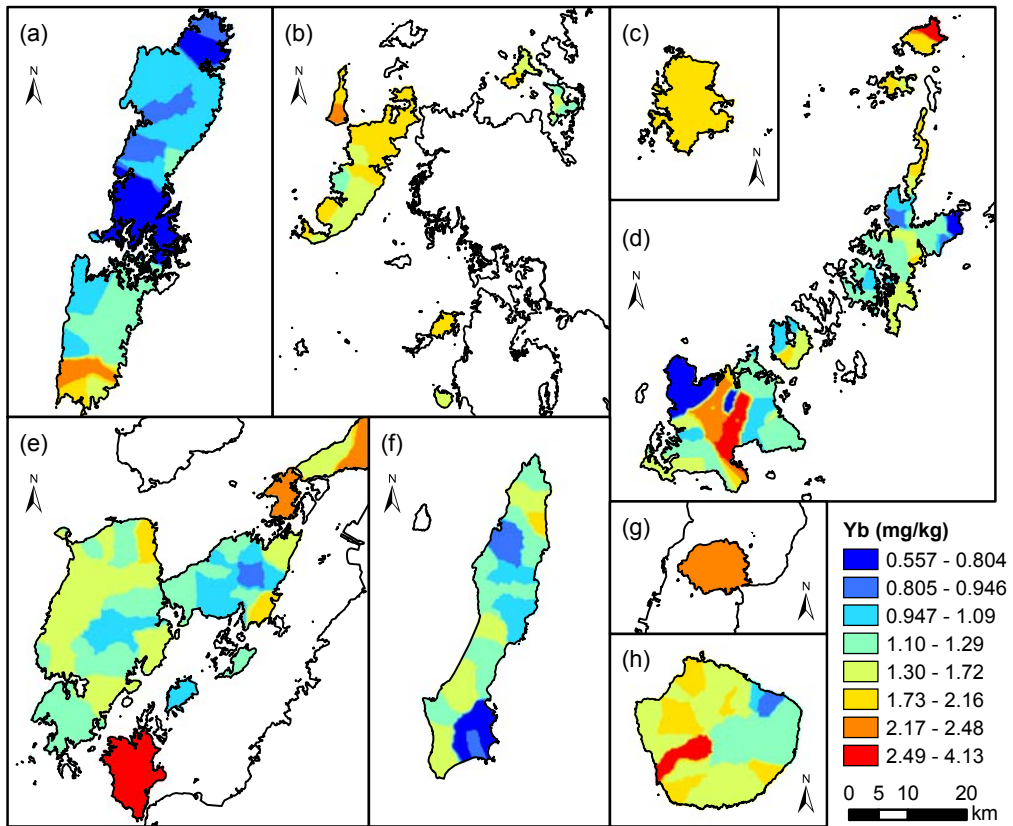
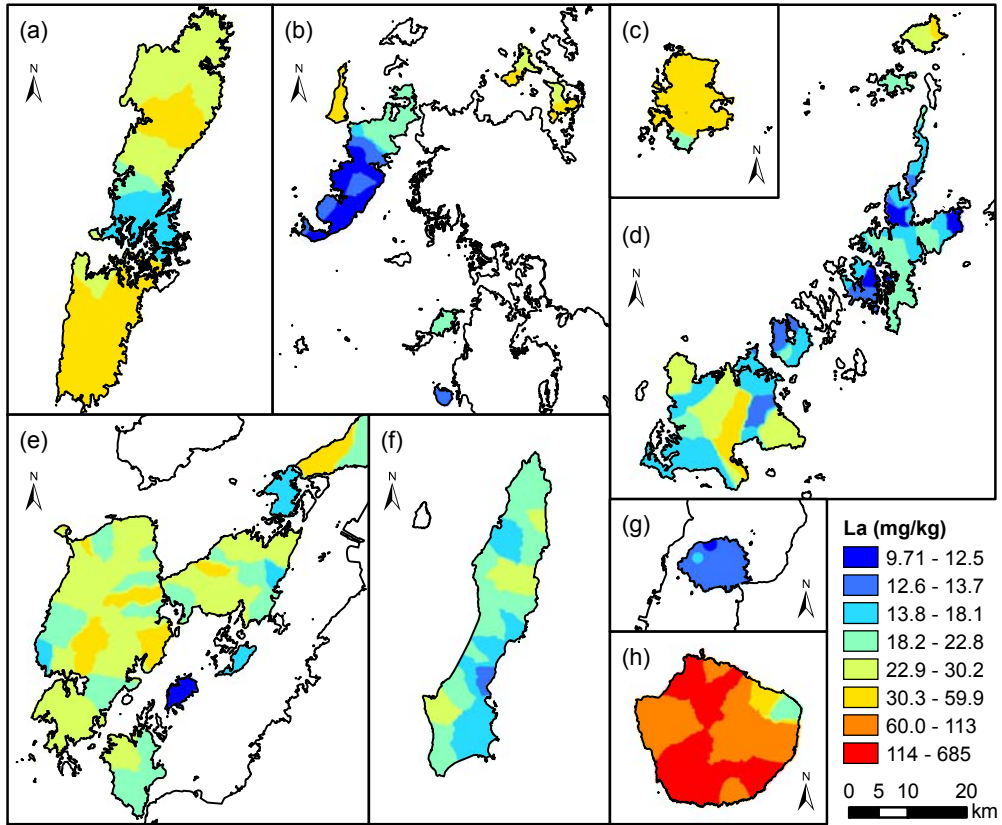


Fig. 8 Spatial distributions of La and Yb concentrations on remote islands. (a)-(h) are the same as Fig. 1.

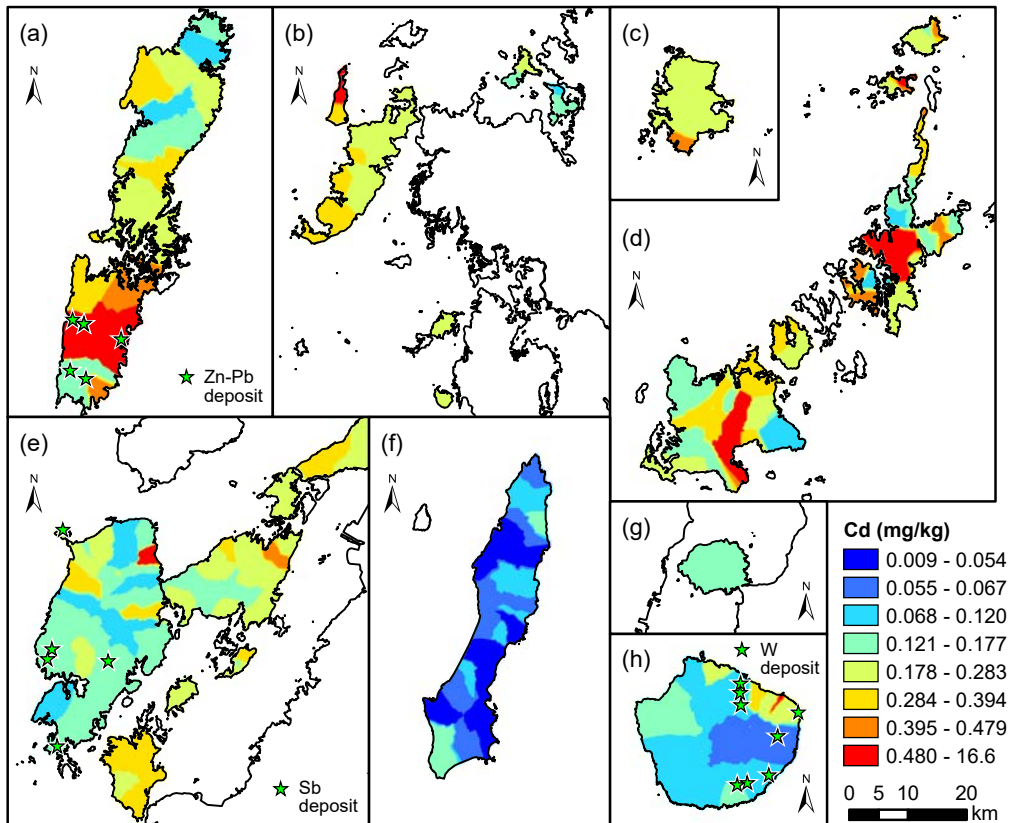
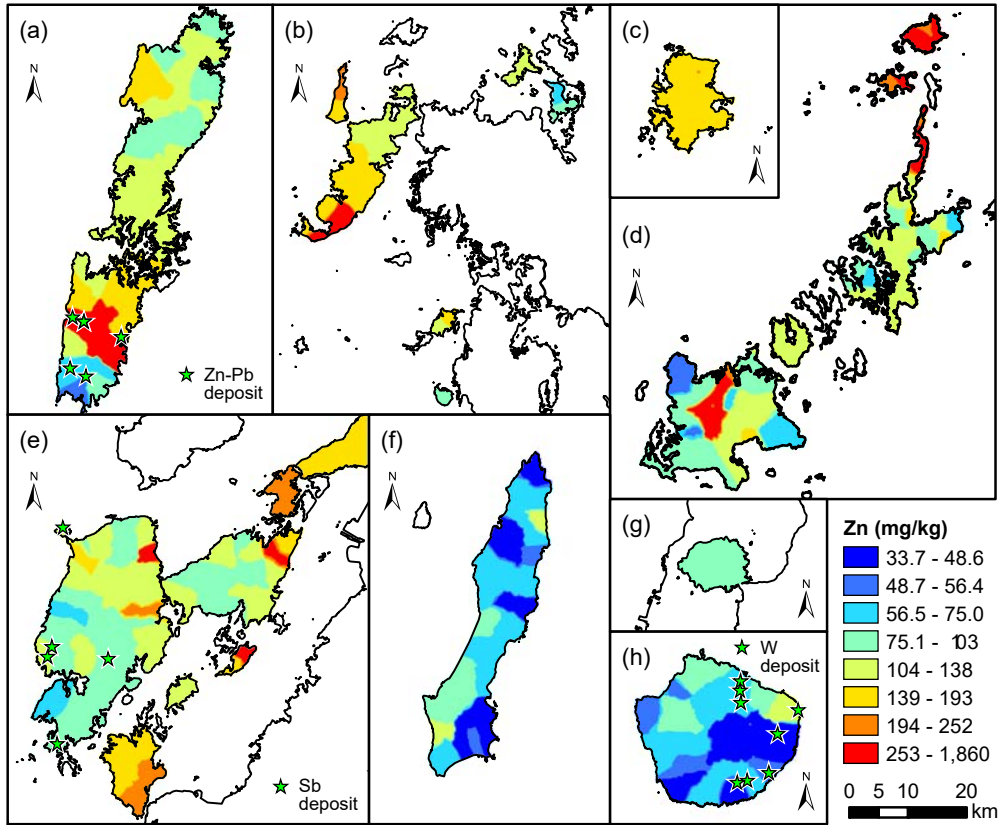


Fig. 9 Spatial distributions of Zn and Cd concentrations on remote islands. Star symbols indicate metalliferous deposits. (a)-(h) are the same as Fig. 1.

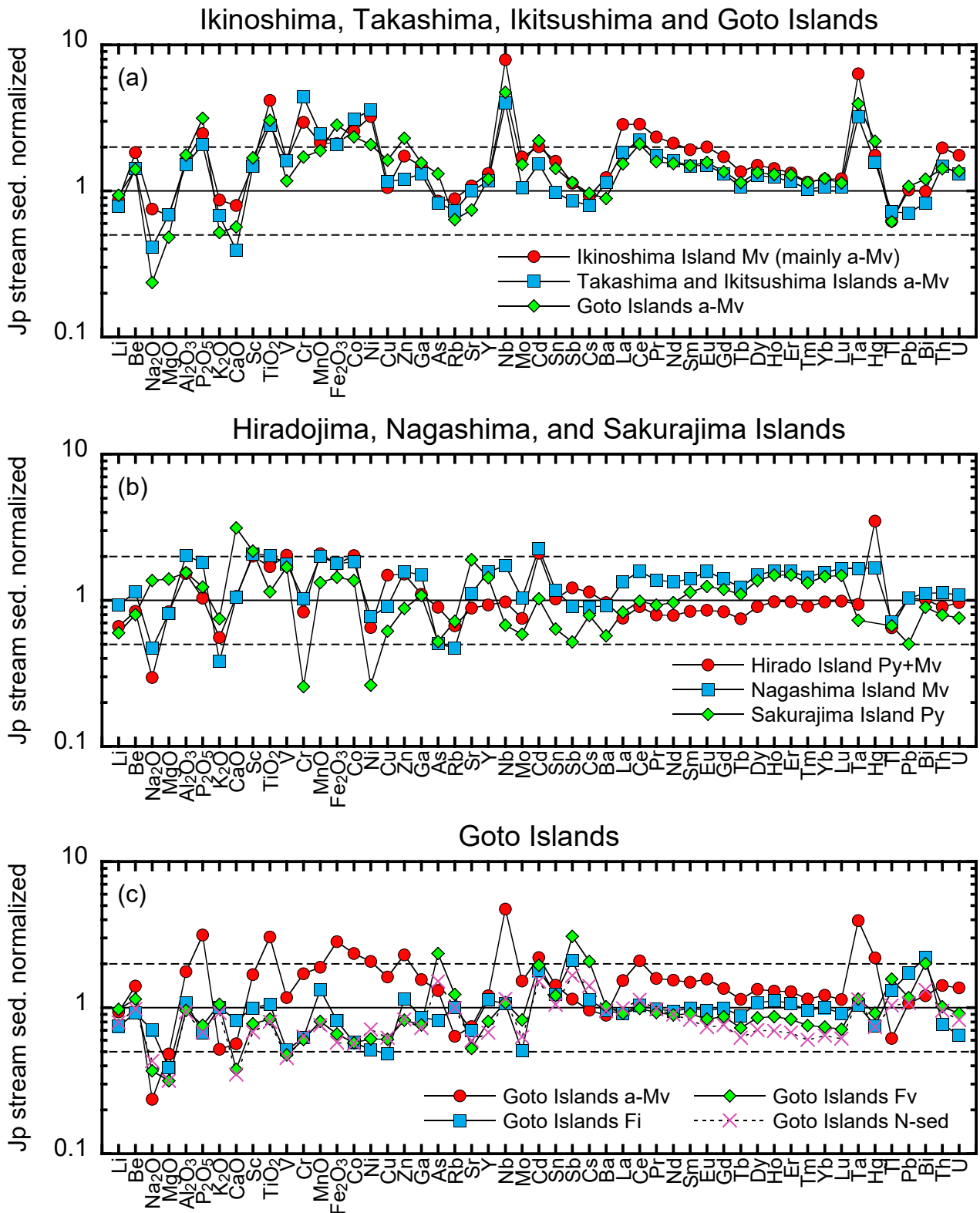


Fig. 10 Chemical composition of stream sediments on isolated islands located in the northern Kyushu region, classified by parent lithology and normalized to median concentrations for Japanese stream sediments, expressed as “Jp stream sed.” Stream sediments (a) on Ikinoshima, Takashima, Ikitsushima, and Goto Islands derived from a-Mv; (b) on Hiradojima, Nagashima, and Sakurajima Islands derived from Mv and Py; (c) on Goto Islands derived from a-Mv, Fv, Fi, and N-Sed. [Abbreviations: a-Mv (alkaline mafic volcanic rock), Mv (non-alkaline mafic volcanic rock), Py (pyroclastic rock), Fi (non-alkaline pyroclastic rock), N-Sed (Neogene sediment)]

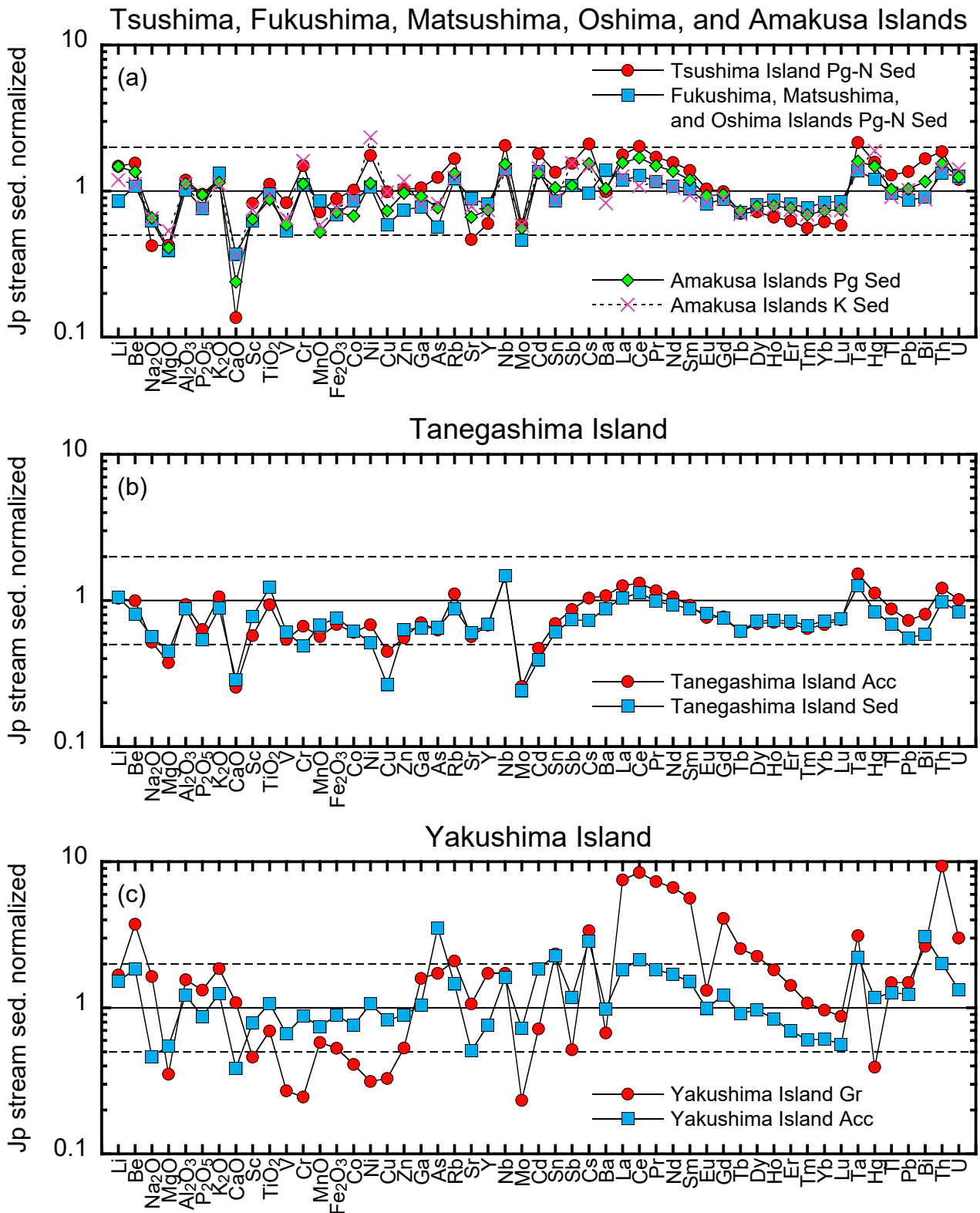


Fig. 11 Chemical composition of stream sediments on (a) Tsushima, Fukushima, Matsushima, Oshima, and Amakusa Islands; (b) Tanegashima Island; and (c) Yakushima Island. Values are classified by parent lithology and normalized to median concentration in Japanese stream sediments, expressed as “Jp stream sed.” [Abbreviations: N-Q Sed (Neogene-Quaternary sediment), Pg-N Sed (Paleogene-Neogene sediment), Pg Sed (Paleogene sedimentary rock), K Sed (Cretaceous sedimentary rock), Acc (accretionary complex), and Gr (granitic rock)]

Cr, Ni, Cu, and Zn, but enriched in Na₂O, MgO, CaO, and Sr, and had a low La/Yb ratio compared to stream sediments from Hiradojima Island and Nagashima Island. These different geochemical abundance patterns in stream sediments are caused by the differences in the chemical and mineralogical compositions of the host rocks.

The Goto Islands (Ukujima, Ojikajima, Nakadorijima, Wakamatsujima, Hisakajima, and Fukuejima) are composed of various lithologies (Fig. 2d and Table 2). Stream sediments derived from Neogene non-alkaline felsic volcanic (Fv) and felsic intrusive (Fi) rocks and Neogene sediment (N Sed) have similar abundance patterns (Fig. 10c). Neogene sediments (Sed) in the Goto Islands were deposited in the Late Oligocene to earliest Middle Miocene, and predate the volcanic activity that occurred during the middle to late Middle Miocene. Therefore, the similar abundance patterns indicate that stream sediments in the Goto Islands are simply a mixture of clastic materials derived from the above three lithologies, although the stream sediments were classified into groups according to their representative lithologies. However, stream sediments derived from alkaline mafic volcanic rock (a-Mv) had an abundance pattern different from those for the other lithologies (Fv, Fi, and N Sed) (Fig. 10c) because alkaline mafic volcanic rocks are geographically separated on Ojikajima and Ukujima Islands and are located at separate ends of Fukuejima Island (Fig. 2d).

Stream sediments derived from unconsolidated sediment and sedimentary rock were collected from isolated islands located in distant places (Fig. 11a). However, their geochemical abundance patterns were similar; they all were poor in Na₂O, MgO, CaO, Sc, and V, and rich in Nb and Ta, and had high La/Yb ratios. On the Amakusa Islands, stream sediments derived from Cretaceous sedimentary rock (K Sed) had a chemical composition very similar to that for Paleogene sedimentary rock (Pg Sed), although there was a lower La/Yb ratio in the former. On Tanegashima Island, the geochemical abundance patterns for stream sediments derived from Paleogene accretionary complex (Acc) resembled those for Neogene-Quaternary sediment (N-Q Sed) (Fig. 11b). These results suggest that sediments deposited during the Neogene-Quaternary age originated from the Paleogene accretionary complex, which is found on both Tanegashima and Yakushima Islands. Stream sediments derived from the accretionary complex (Acc) on Yakushima Island had abundance patterns similar to those for the accretionary complex in Tanegashima Island but at greater concentrations (Figs. 11b, c). Sandstone and alternating sandstone and mudstone, a *mélange* matrix, are the dominant facies on both Tanegashima Island and Yakushima Island (Kawanabe *et al.*, 2004; Saito *et al.*, 2007). However, the exposed areas of mudstone and mud-dominated turbidite in the drainage basins for the Tanegashima and Yakushima samples were 6–27% (10% of median value) and 15–61% (30% of median value), respectively. Consequently, the lower concentrations of

elements in the Tanegashima samples must be caused by the dilution effect of quartz because sandstone is more abundant in quartz than in mudstone. Neogene granitic rock that had intruded into the central part of Yakushima Island greatly elevated the Li, Be, Na₂O, CaO, Sr, Y, Ln, Th, and U concentrations in stream sediments, and reduced the MgO, Sc, TiO₂, V, Cr, MnO, T-Fe₂O₃, Co, Ni, Cu, and Zn concentrations (Fig. 11c). The enrichment by Na₂O, CaO, and Sr can be explained by the large amount of plagioclase in stream sediments. The extreme enrichment with Li, Be, Y, Ln, Th, and U was caused by excess accumulation of accessory minerals, such as beryl and monazite, in the fine sand fraction as shown in Fig. 4.

5. Summary

A total of 193 stream sediments were collected from 22 remote islands around Kyushu Island and Uto Peninsula, and 3 volcanic ash deposits were collected from Sakurajima Island. The concentrations of 53 elements in these samples were determined using ICP-AES, ICP-MS, and AAS. The results indicated that 12, 9, 31, 20, and 19 of the stream sediments were derived predominantly from alkaline mafic volcanic rock, Cretaceous sedimentary rock, Paleogene sedimentary rock associated with coal mines, and Neogene granitic rock, respectively. These rock types represent a limited number of outcrops on mainland Japan. The remainder of the samples originated from Neogene-Quaternary sediments, non-alkaline mafic volcanic and pyroclastic rocks, and Paleogene accretionary complexes.

The variation in element concentration with grain size was determined for Sk03, Tn02, Tn09, Tn26, Yk01, and Yk17. The concentrations of many elements in Sk03 showed little change with grain size because sand-sized particles were composed of agglutinated silt-sized volcanic ash. The concentrations of many elements in the remainder of the samples decreased with decreasing grain size from the very coarse sand fraction, reached a minimum for the fine sand fraction, and then increased as the grain size further decreased, resulting in a V-shaped pattern.

Stream sediments derived from mafic volcanic and pyroclastic rocks and volcanic ash deposits were enriched with Al₂O₃, MgO, CaO, P₂O₅, Sc, TiO₂, V, MnO, T-Fe₂O₃, Co, Cu, Zn, and Sr. Alkaline mafic volcanic rock contained highly elevated concentrations of Cr, Ni, Nb, La, Ce, Pr, Nd, and Ta in stream sediments. The stream sediments from Yakushima Island, which are mostly underlain by Neogene granitic rock, were extremely abundant in Be, Na₂O, K₂O, CaO, Sr, Y, Ln, Th, and U. These enrichments can be explained by the large amount of plagioclase and K-feldspar and by accumulation of accessory minerals such as apatite and monazite. Cretaceous–Paleogene sedimentary rocks and Paleogene–Neogene sediments were distributed discretely on Tsushima, Fukushima, Matsushima, Oshima, and Amakusa-kamishima, Amakusa-shimoshima, Goshorajima, and Shishijima Islands.

Nevertheless, stream sediments derived from these rocks had similar geochemical abundance patterns. Furthermore, except for Cr, Ni, and heavy metals, the geochemical abundance patterns for stream sediments originating from Cretaceous-Paleogene sedimentary rocks and Paleogene-Neogene sediments resembled those from Paleogene accretionary complex distributed on Tanegashima and Yakushima Islands. These results suggest that the accretionary and non-accretionary sedimentary rocks have a common origin. Thus, geochemical features of stream sediments on isolated islands are strongly influenced by the parent lithology in their watershed. Finally, although a number of a large-scale metalliferous deposits were limited to remote islands, enrichment with Zn, Cd, and Pb in stream sediments was found near the Zn-Pb mine on Tsushima Island. Similarly, Sb concentrations were significantly greater in stream sediments collected near the Sb mine on Amakusa-shimoshima Island.

Acknowledgement

Sampling in Yakushima Island National Park was conducted with the permission and cooperation of the Yakushima Ranger Office, Ministry of the Environment, Yakushima Forest Management Office, Kyushu Regional Forest Office, and Yakushima Forest Ecosystem Conservation Center.

References

- Darnley, A. G., Björklund, A., Bølviken, B., Gustavsson, N., Koval, P. V., Plant, J. A., Steinfeld, A., Tachid, M., Xie, X., Garrett, R. G. and Hall, G. E. M. (1995) *A global geochemical database for environmental and resource management: recommendations for international geochemical mapping*. UNESCO Publishing, Paris, 122p.
- Geological Survey of Japan, AIST (ed.) (2015) *Seamless digital geological map of Japan 1: 200,000. May 29, 2015 version*. Geological Survey of Japan, AIST.
- Howarth, R. J. and Thornton, I. (1983) Regional Geochemical Mapping and its Application to Environmental Studies. In Thornton, I., ed., *Applied Environmental Geochemistry*, Academic Press, London, 41–73.
- Imai, N. (1987) Multielement analysis of stream sediment by ICP-AES. *Bunseki Kagaku*, **36**, T41–T45 (in Japanese with English abstract).
- Imai, N. (1990) Multielement analysis of rocks with the use of geological certified reference material by inductively coupled plasma mass spectrometry. *Anal. Sci.*, **6**, 389–395.
- Imai, N., Terashima, S., Itoh, S. and Ando, A. (1995) 1994 compilation of analytical data for minor and trace-elements in 17 GSJ geochemical reference samples, igneous rock series. *Geostand. Newsl.*, **19**, 135–213.
- Imai, N., Terashima, S., Itoh, S. and Ando, A. (1996) 1996 compilation of analytical data on nine GSJ geochemical reference samples, “Sedimentary rock series”. *Geostand. Newsl.*, **20**, 165–216.
- Imai, N., Terashima, S., Ohta, A., Mikoshihara, M., Okai, T., Tachibana, Y., Togashi, S., Matsuhisa, Y., Kanai, Y., Kamioka, H. and Taniguchi, M. (2004) *Geochemical map of Japan*. Geological Survey of Japan, AIST, 209p.
- Imai, N., Terashima, S., Ohta, A., Mikoshihara, M., Okai, T., Tachibana, Y., Togashi, S., Matsuhisa, Y., Kanai, Y. and Kamioka, H. (2010) *Geochemical Map of Sea and Land of Japan*. Geological Survey of Japan, AIST, 207p.
- Imai, N., Okai, T., Ohta, A., Mikoshihara (Ujiie), M., Kanai, Y., Kubota, R., Tachibana, Y., Terashima, S., Ikehara, K., Katayama, H. and Noda, A. (2015) *Geochemical Map of Kanto Region*. Geological Survey of Japan, AIST, 217p.
- Karakida, Y., Hayasaka, S. and Hase, Y. (1992) *Regional Geology of Japan Part 9 (KYUSHU)*. Kyoritsu Shuppan Co., 354p.
- Kawanabe, Y., Sagaguchi, K., Saito, M., Komazawa, M. and Yamazaki, T. (2004) *Geological Map of Japan 1:200,000, Kaimon Dake and a part of Kuro Shima*. Geological Survey of Japan, AIST.
- Minami, M., Jomori, Y., Suzuki, K. and Ohta, A. (2017) Grain-size variations in $^{87}\text{Sr}/^{86}\text{Sr}$ and elemental concentrations of stream sediments in a granitic area: Fundamental study on $^{87}\text{Sr}/^{86}\text{Sr}$ spatial distribution mapping. *Geochem. Jour.* **51**, 469–484.
- Ohta, A. (2018) Evaluation of straightforward and rapid multi-element analyses of stream sediments for geochemical mapping in the remote islands of Japan — Seto Inland Sea region —. *Bull. Geol. Surv. Japan*. **69**, 1–30.
- Ohta, A., Imai, N., Terashima, S., Tachibana, Y., Ikehara, K. and Nakajima, T. (2004) Geochemical mapping in Hokuriku, Japan: influence of surface geology, mineral occurrences and mass movement from terrestrial to marine environments. *Appl. Geochem.*, **19**, 1453–1469.
- Reimann, C. (2005) Geochemical mapping: technique or art? *Geochem.: Explor. Environ. Anal.*, **5**, 359–370.
- Saito, M., Ogasawara, M., Nagamori, H., Geshi, N. and Komazawa, M. (2007) *Geological Map of Japan 1:200,000, Yaku shima*. Geological Survey of Japan, AIST.
- Shimazu, H. and Nishi, K. (2004) Distribution of maximum diameter of riverbed sediments and debris transport processes in Yakushima Island, Southern Jap. *Bull. Geo-environmental Sci.* **6**, 131–137 (in Japanese).
- Terashima, S. (1976) The determination of arsenic in rocks, sediments and minerals by arsine generation and atomic absorption spectrometry. *Anal. Chim. Acta*, **86**, 43–51.
- Terashima, S. (1984) Determination of arsenic and antimony in geological-materials by automated hydride generation and electrothermal atomic-absorption spectrometry. *Bunseki Kagaku*, **33**,

561–563 (in Japanese with English abstract).
Terashima, S., Imai, N., Ikehara, K., Katayama, H., Okai, T., (Ujiie) Mikoshiba, M., Ohta, A. and Kubota, R. (2008) Variation of elemental concentrations of river and marine sediments according to the grain size classification. *Bull. Geol. Surv. Japan*, **59**, 439–459 (in Japanese with English abstract).

Webb, J. S., Thornton, I., Thompson, M., Howarth, R. J. and Lowenstein, P. L. (1978) *The Wolfson Geochemical Atlas of England and Wales*. Clarendon Press, Oxford, 69p.

Received December 26, 2017

Accepted October 23, 2018

九州離島域の地球化学図作成

太田充恒

要 旨

本論文では、西南日本離島域を対象とした高密度地球化学図についての報告を行う。九州地方の陸海域地球化学図や現在作成中の広域Sr同位体図における研究調査を補完し強化する事を目的として、193試料の河川堆積物および3試料の火山灰降下堆積物を主に九州周辺の離島から採取し、53元素の分析を行った。堆積物試料中の元素広域分布と地質との関係を地理情報解析ソフトウェアを用いて詳細に調べた。非アルカリ苦鉄質火山岩や火砕岩由来の河川堆積物や火山灰降下堆積物はマグネシウム、カルシウム、スカンジウム、チタン、バナジウム、鉄、コバルト、ストロンチウムに富んでいた。アルカリ苦鉄質火山岩はさらに河川堆積物中のクロム、ニッケル、ニオブ、ランタン、セリウム、プラセオジウム、ネオジウム、タンタル濃度も増加させた。花崗岩由来の河川堆積物は、ベリリウム、ナトリウム、カリウム、カルシウム、ストロンチウム、イットリウム、ズズ、ランタノイド元素、トリウム、ウランに富んでいた。付加帯・非付加帯堆積岩は河川堆積物中のニオブやタンタル濃度を増加させたが、ナトリウム、マグネシウム、カルシウム、ストロンチウム濃度を低下させた。これらの地球化学的な特徴は、碎屑物中の母岩から供給された主要造岩鉱物（例えば石英、斜長石、カリ長石、苦鉄質鉱物）や副成分鉱物（例えば、アパタイトやモナザイト）の相対的な存在量によって説明が可能である。また、亜鉛・鉛鉱床が対馬の河川堆積物中の亜鉛、カドミウム、鉛濃度を高め、アンチモン鉱床が天草下島の河川堆積物中のアンチモン濃度を高めたことが確認された。

